**Atmospheric
Chemistry
and Physics
Discussions**

ACPD

4, 7917–7984, 2004

Hydrological cycle of
MATCH

R. Lang and
M. G. Lawrence

Evaluation of the hydrological cycle of MATCH driven by NCEP reanalysis data: comparison with GOME water vapor field measurements

R. Lang and M. G. Lawrence

Max-Planck Institute for Chemistry, Mainz, Germany

Correspondence to: R. Lang (lang@mpch-mainz.mpg.de)

EGU

Abstract

This study examines two key parameters of the hydrological cycle, water vapor (WV) and precipitation rates (PR), as modelled by the chemistry transport model MATCH (Model of Atmospheric Transport and Chemistry) driven by National Centers for Environmental Prediction (NCEP) reanalysis data (NRA). For model output evaluation we employ WV total column data from the Global Ozone Monitoring Experiment (GOME) on ERS-2, which is the only instrument capable measuring WV on a global scale and over all surface types with a substantial data record from 1995 to the present. We find that MATCH and NRA WV and PR distributions are closely related, but that significant regional differences in both parameters exist in magnitude and distribution patterns when compared to the observations. We also find that WV residual patterns between model and observations show remarkable similarities to residuals observed in the PR when comparing MATCH and NRA output to observations comprised by the Global Precipitation Climatology Project (GPCP). We conclude that deficiencies in model parameters shared by MATCH and NRA, like, for example, in the evapotranspiration rates, are likely to lead to the observed differences. Regional differences between MATCH modelled WV columns and the observations can be as large as 2 cm on the basis of a three years monthly average. Differences in the global mean WV values are, however, below 1 mm. Regional differences in the PR between MATCH and GPCP can be above 5 mm per day and MATCH computes on average a higher PR than what has been observed. As a consequence, this leads to shorter model WV residence times by about 1 day as compared to NRA data and the observations. We find that MATCH has problems in modelling the WV content in regions of strong upward convection like, for example, along the Inter Tropical Convergence Zone, where it appears to be generally too dry as compared to the observations. The study therefore suggests that a too rapid conversion of WV to precipitate in MATCH, especially in instances of strong convection, leads to regionally too dry model results and in turn to generally too low WV residence times. The study additionally demonstrates the value of the GOME WV

EGU

record for model evaluation.

1. Introduction

The accurate knowledge of the 3-D water vapor (WV) field is essential for the understanding of a variety of physical and chemical processes in the atmosphere and therefore one of the key parameters for the accurate modelling of climate forcing and its feedback mechanisms. WV is the strongest greenhouse gas, because it is the fourth most abundant atmospheric constituent absorbing over large parts of the spectral region from the visible up to the infra-red, and because of its emission of thermal radiation from the far infrared to the microwave regions (Learner et al., 2000). WV plays an essential role in the direct and indirect effect of radiative forcing via its influence on aerosol optical properties and the formation of clouds and precipitation. WV is a driving parameter in reactive chemistry related to ozone and HO_x. Due to its complex spectroscopic structure the contribution of WV to the total radiative forcing budget and the various feedback processes, however, still can not be quantified accurately (Maurellis and Tennyson, 2003; Minschwander and Desseler, 2004). Detailed parameterizations of aerosol optical properties and cloud formation in general circulation models (GCM) and chemical transport models (CTM) are currently being developed (e.g. in the framework of the EU funded Particles of Human Origin Extinguishing Natural solar radiation In Climate Systems project PHOENICS, or the Global Aerosol Model interCOMparison project AEROCOM), but will significantly increase the demand for accurate knowledge of the 3D-WV distribution in the near future (Metzger et al., 2002), as well as the demand for data for cross-comparison and model performance evaluation.

Comparisons of global model output to observations of the atmospheric WV distribution from both GCMs and CTMs are still in their early stages due to lack of independent and consistent observations with global coverage on longer time scales. This paper and a following companion paper will therefore address the question how well the hydrological cycle is represented by a CTM frequently used for modelling of tropospheric

R. Lang and
M. G. Lawrence

Title Page

Abstract	Introduction
Conclusions	References
Tables	Figures

◄◄ ►►

◄ ►

Back Close

Full Screen / Esc

Print Version

Interactive Discussion

[EGU](#)

Hydrological cycle of MATCH

R. Lang and
M. G. Lawrence

ozone and aerosol related chemistry: The Model of Atmospheric Transport and Chemistry (MATCH). MATCH is, as other CTMs, driven by basic meteorological input data, i.e. temperature, pressure, horizontal winds, surface wind stresses, and latent and sensible heat fluxes, which are taken from weather center analysis and re-analyses, such

5 as those from the National Centers for Environmental Prediction (NCEP) or the European Center for Medium-range Weather Forecasts (ECMWF). However, in contrast to other CTMs, MATCH is currently, to the best of our knowledge, the only CTM where the tropospheric hydrological cycle is calculated directly within the model, using NCEP surface evapotranspiration fluxes as the input of WV to the troposphere and employing

10 parameterizations for cloud formation and precipitation, which are closely related to those used in the Community Climate Model version 3 (CCM3) of the National Center for Atmospheric Research (NCAR). MATCH may therefore be characterized as what we call a "semi-online" CTM. This specific formulation of the MATCH model guarantees a consistent balance between evaporation fluxes and precipitation rates (PR), and

15 prevents an under or overestimation of the atmospheric WV residence time via a too rapid or too slow conversion of nudged specific humidity in precipitation.

The question posed by this paper is how well are the main parameters of the hydrological cycle represented by MATCH over longer time series in comparison to data-assimilation models like the ECMWF REanalysis ERA-40 (ERA) and the NCEP/NCAR

20 Reanalysis (NRA). The paper focuses on the evaluation of modelled monthly mean WV content and precipitation amounts computed by MATCH driven by NRA. MATCH has been used for numerous studies of atmospheric chemistry and transport including the chemistry of tropospheric ozone and nonmethane hydrocarbons (Rasch et al., 1997; Mahowald et al., 1997a,b; Lawrence and Crutzen, 1998, 1999; Lawrence, 2001;

25 Lawrence et al., 1999, 2003a; von Kuhlmann et al., 2003a,b; Bonn et al., 2004; Kunhikrishnan et al., 2004a,b,c; Labrador et al., 2004a,b), and for chemical weather forecasting using NCEP Analysis data (Lawrence et al., 2003b). Differences between model output and observations are analyzed in light of the previously mentioned ongoing studies on new aerosol and cloud microphysical parameterizations used in models which only

Hydrological cycle of MATCH

R. Lang and
M. G. Lawrence

Title Page

Abstract | Introduction

Conclusions | References

Tables | Figures

|◄ | ►|

◄ | ►

Back | Close

Full Screen / Esc

Print Version

Interactive Discussion

EGU

may successfully be evaluated providing a good understanding of all other parameters and mechanism leading to the observed residuals. The evaluation of the modelled WV distribution requires appropriate observations on a global scale, preferably from independent sources, which also can be cross-evaluated to help reveal where model

5 discrepancies appear robust in light of measurement errors. The second main purpose of this study is to present such a set of observations, which we will use to evaluate various configurations of MATCH as well as of the GCM ECHAM version 5 in subsequent studies.

MATCH and NRA WV distributions will be compared to independent satellite based

10 remote sensing measurements from the Global Ozone Monitoring Experiment (GOME) on ESA's ERS-2 satellite platform covering the whole globe. GOME WV data retrievals have recently be demonstrated to deliver good results over all surface types and in cloud-free situations (Lang et al., 2003). GOME data is not assimilated in either ERA or NRA and provides a data record starting in August 1995 until present, which makes

15 it suitable for model evaluations. The evaluated data periods cover August 1996 to 1998 and January 1996 to 1998, including the strong ENSO years of 1997 and 1998. There is no other instrument with a comparable data record measuring WV on a global scale and over all surfaces types. Well known instrument suites like the TIROS Operational Vertical Sounder (TOVS) and is successors (Advanced-TOVS series; 1979 to

20 present), or the Special Sensor Microwave Imager (SSM/I) on the Defense Meteorological Satellite Platform (DMSP) series (1987 to present) measure WV in the infrared or microwave regions and are restricted to either land or ocean surfaces (Engelen and Stephens, 1999). New generations of instruments like the Moderate Resolution Imaging Spectroradiometer (MODIS) on the Aqua and Terra platforms (1999–present),

25 the Medium Resolution Imaging Spectrometer (MERIS) and the SCanning Imaging Absorption spectroMeter for Atmospheric CartograpHY (SCIAMACHY) on ESA's EN-VISAT (2002 to present), as well as the instruments more specifically dedicated to WV like the Atmospheric Infrared Sounder (AIRS; 2002 to present) on Aqua and the Infrared Atmospheric Sounding Interferometer (IASI) to be launched by the end of 2005

on EUMETSATs Metop series, will greatly improve our knowledge of the tropospheric 3-D WV field. However, the data record of most of the named instruments is not yet long enough for valuable model evaluations. It should also be mentioned, that even though significant advances in remote sensing technology have been made in recent years and instruments like AIRS and IASI will achieve unprecedented spatial resolution performances, in order to get the complete knowledge of the 3-D WV distribution a combination of data from various sensors as well as radiosondes will still be required within the foreseeable future. This study will demonstrate the value as well as the limitations of the GOME WV data record and that of its successors (GOME-2 on the METOP series) to contribute to blended WV products for model evaluation.

In Sect. 2 we describe the various sources used for MATCH model output evaluation starting with a detailed description of the GOME WV product (Sect. 2.1). This is the first use of the GOME WV-record for model evaluation. A brief description of the applied Spectral Structure Parameterization (SSP) algorithm developed by Maurellis et al. (2000a) and Lang et al. (2003) for retrieval of narrow band absorbers will be provided together with a more detailed description of the simultaneously derived cloud-mask (Sect. 2.2). The latter is crucial for instruments measuring tropospheric constituents in the near-infrared, the visible and the UV region of the spectrum like WV or NO_2, for which the total columns retrieved are significantly affected by clouds blocking the light from travelling through the lower region of the atmosphere. Satellite based WV measurements from SSM/I briefly described in Sect. 2.3 are used together with radiosonde data to demonstrate the feasibility of using GOME WV data for model evaluations over ocean and land surfaces. The NASA Water Vapor Project (NVAP) data set introduced in Sect. 2.4 combines WV data from SSM/I, the TOVS instruments, and radiosonde data to provide a product for model evaluation and climate studies on a global scale. We use NVAP data as an additional source for comparison of both model output data and data retrieved from GOME. Note, however, that NVAP is not a completely independent source for transport model evaluations because both SSM/I and TOVS data are routinely assimilated in weather center reanalysis products. The meteorological input

EGU

Hydrological cycle of MATCH

R. Lang and
M. G. Lawrence

parameters from NRA used in MATCH will be discussed in Sect. 4 for their crucial influence on the MATCH hydrological cycle and the specific implementation of the MATCH model employed here is laid out in Sect. 5.

After a detailed evaluation of the GOME WV record over the three years period of interest in Sect. 6.1 we compare monthly averaged WV fields computed by MATCH for different periods with results from GOME, NVAP and NRA in Sect. 6.2. Therein, residuals between rain gauges measurements compiled by the Global Precipitation Climatology Project (GPCP) (Rudolf, 2001) (for a description of the GPCP data set see Sect. 3) and model as well as reanalysis fields, will be compared to derived residuals from comparisons of model WV fields with GOME measurements. We will focus on regions like Europe and the Southern Asian/Indian Ocean area, which are of specific interest with respect to the impact of anthropogenic and non-anthropogenic aerosol load on the parameters of the hydrological cycle. The results will be discussed in order to differentiate between MATCH model-related effects on the observed residual patterns and differences caused by the influence of reanalysis data contribution on the model results. We will finally draw conclusions which will provide a basis for following-up MATCH model sensitivity studies using different sets of reanalysis data and different assumptions in the basic parameters.

2. Water vapor measurements

2.1. GOME

The Global Ozone Monitoring Experiment (GOME) spectrometer on the European Space Agency's ERS-2 satellite (ESA, 1995; Burrows et al., 1999) measures backscattered solar radiation continuously between between 240 and 790 nm with a spectral resolution of on average 0.22 nm in the visible and near infrared regions. Column concentration retrieval is routinely carried out for O_3 and NO_2 (level 2 products). Important information about OClO, volcanic SO_2, CH_2O from biomass burning and tropospheric

BrO, has also been delivered (Thomas et al., 1998). The instrument measures on a spatial resolution of 40 by 320 km at three different observation angles, west, nadir and east scanning, resulting in a total swath width of 960 km. ERS-2 crosses the equator at about 10:30 local time. The absorption spectra derived from channel 3 and 4 of the instrument contain 3 overtone absorption bands of WV around 580, 640 and 720 nm. Measurements presented here make use of the 580 nm absorption band covered by 185 detector pixels between 560 and 600 nm. This spectral region also contains additional broad-band absorption features of the O_3 Chappuis absorption band and a strong absorption by $(O_2)_2$ (see Fig. 1)(Lang et al., 2002). The forward model employed is the Spectral Structure Parameterization (SSP) model (Maurellis et al., 2000a; Lang et al., 2003) including direct-surface and single-scattering path contribution. SSP already demonstrated its capability to derive total water vapor column (WVC) values over all surface types in cloud-free situation with an accuracy of 0.3 cm for moderate aerosol-impact scenarios based on more than 300 representative GOME retrievals and 0.5 cm in aerosol rich environments. So far, WVC from the GOME instrument has been derived for specific case studies only (Noël et al., 1999; Noël et al., 2002; Maurellis et al., 2000b; Casadio et al., 2000; Wagner et al., 2003; Lang et al., 2002, 2003), which have not yet demonstrated their potential for transport model evaluation over longer time series. Apart from providing WVC over all surface types and in cloud-free situations, GOME WVC are an independent measurement validation from water vapor fields delivered by the NCEP or ECMWF reanalysis set, which are frequently used for data assimilation or evaluation in CTMs. In contrast, SSM/I and (A)TOVS WVC are routinely assimilated in the mentioned reanalysis sets. The coarse spatial resolution is one of the major disadvantages of the GOME data set, resulting in a significant amount of ground pixels identified as being affected by clouds and therefore having to be removed from the analysis. However, with its now more than nine years record of data the instrument data set is well suited for the evaluation of model-parameters from transport models or even from general circulation model output, where usually monthly averaged quantities of more than six to seven years are required for meaningful climatological comparisons

Title Page

Abstract | Introduction

Conclusions | References

Tables | Figures

|◀ | ▶|

◀ | ▶

Back | Close

Full Screen / Esc

Print Version

Interactive Discussion

EGU

with measured data.

2.2. GOME cloud mask

The quality of the detection of clouds within the observed slant path is a crucial criterium for the quality of tropospheric retrievals from instruments measuring in the visible and infrared region. Clouds may alter the retrieved total column results in two ways: either by blocking the light from travelling through the lower regions of the atmosphere leading, in case of WV, to a reduced total column retrieval, or by increasing the path length due to multiple scattering inside or at the cloud edges, which may in contrast lead to an increased column retrieval depending on cloud height and geometry. Advanced cloud detection schemes of nadir viewing instruments delivering information about cloud top height and cloud fraction (fraction of the ground pixel covered by clouds) may also be used to deliver some profile information about the atmospheric species under study (Albert et al., 2001). Here, we focus on the accuracy of the total column value and therefore the accuracy of the derived cloud mask removing pixels from the analysis, where the occurrence of clouds leads to a deviation of retrieved WVC value from the real one. Figure 1 shows the atmospheric reflectivity spectrum between 565 and 600 nm as seen by GOME. Besides the two absorption features of the 5ν-polyad WV overtone band around 570 and 592 nm also the broad absorption feature by the oxygen collision complex $(O_2)_2$ with a maximum absorption around 577 nm is clearly visible. This feature is used for each retrieval to evaluate the averaged traversed air-mass by all photons detected for an individual GOME pixel scan (Pfeilsticker et al., 1997; Wagner et al., 2003). The retrieval algorithm employs pressure and temperature profiles from the Neutral Atmosphere Empirical Model NRLMSISE-00 (Picone et al., 2002) for altitude-layer dependent calculations of cross-sections, the calculation of Rayleigh single scattering albedo and the calculation of geometrical air-mass factors depending on the measurement geometry. Pressure dependent cross-sections for $(O_2)_2$ are provided by (Naus and Ubachs, 1999). From the relation between the geometrical air-mass factor and the observed one, as derived from the $(O_2)_2$ absorp-

EGU

tion, a pixel averaged cloud top pressure can be derived, which is used here as the primary cloud detection criterium (SSP-$(O_2)_2$ retrieval scheme). Two additional secondary criteria are used in order to decide if a pixel is marked as cloud covered as opposed to cloud free. One is a ground-pixel-averaged albedo value larger than 0.1, spectrally averaged between 560 and 600 nm and the second is a flat or decreasing spectral dependency of the albedo with respect to wavelength. The latter criterium distinguishes desert pixels with bright surfaces and increasing albedo (with wavelength) in this specific region of the spectrum (Koelemeijer et al., 1997) from white or grey cloud surfaces. In cases where the primary air-mass factor derives a pixel averaged cloud top-height of 500 m above the ground and the two secondary criteria are satisfied, the ground pixel is marked as affected by clouds and removed from the retrieval results.

We evaluate the performance of this cloud masking scheme by comparison with corresponding cloud masks and cloud top pressures as derived from the Fast Retrieval Scheme for Cloud from the Oxygen A-band (FRESCO)(Koelemeijer et al., 2001). FRESCO is based on non-linear least squares fitting of the GOME reflectivity measured around the oxygen A-band (758–778) in order to derive cloud top pressures and cloud fraction from the GOME instrument. The cloud albedo is fixed to 0.8 resembling an optically thick cloud. FRESCO derived CTP and cloud fraction should therefore be seen as effective numbers. Comparisons between FRESCO and independent satellite cloud products like monthly averaged values from the International Satellite Cloud Climatology Project (ISCCP)(Rossow and Schiffer, 1991) reveal a bias in the FRESCO derived CTP of around 50 hPa lower cloud tops and with comparable standard deviation, which has been identified as a result of neglecting the absorption of oxygen within and below the cloud. FRESCO has already successfully been used in a number of applications retrieving tropospheric constituents from GOME and tested in additional inter-comparison studies confirming largely the above cited results (Tuinder et al., 2004). FRESCO data from GOME is generated and provided by the SCIAMACHY data center (http://neonet.knmi.nl/neoaf/).

Figure 2 shows a comparison between CTP derived by FRESCO and the SSP-$(O_2)_2$

EGU

retrieval scheme. FRESCO CTP values are weighted by the FRESCO cloud-fraction in order to provide comparable ground-pixel averaged CTP values. The figure indicates a good correlation between both retrieval schemes, although FRESCO sees on average higher clouds than SSP-$(O_2)_2$. However, for the construction of an operational cloud mask, as required here, it is necessary to introduce an empirical limit in cloud fraction or cloud top height, which has been evaluated to affect the retrieved column quantities only to an extent below or of the order of other quantified retrieval errors. From previous studies, we evaluated the influence of a 15% cloud cover on the retrieved column to be on average below other retrieval biases (Lang et al., 2003). Figure 3 compares the cloud mask derived from FRESCO on 1 August 1998, applying a 15% cloud cover fraction limit, with the cloud mask derived from SSP-$(O_2)_2$. For the SSP-$(O_2)_2$ applied limits laid out above, both cloud mask retrievals compare very well except for desert regions, where FRESCO is known to deliver significantly larger cloud fraction values as observed from other cloud-retrieval schemes (Grzegorski, 2003). In contrast, SSP-$(O_2)_2$ observes the Saharan region, together with the Near East and the Gobi desert, as expected as being predominantly cloud free.

2.3. SSM/I

The Special Sensor Microwave/Imager (SSM/I) (Hollinger et al., 1990) has been in orbit since 1987 on various platforms, predominantly of the Defense Meteorological Space Programs (DMSP) F-platform series. For the purpose of this study we use data from the F-13 and F-14 platforms in an near circular, sun-synchronous, and near-polar orbit with an inclination of 98.8° at an altitude of about 850 km and an orbital period of 102 min. F-13 and F-14 were launched in 24 March 1995 and 4 April 1997 and cross the equator at 06:15 and 08:20 local time, respectively. SSM/I data from these platforms can be correlated with GOME data within 4 and 2 h (ERS-2 equator crossing at 10:30 LT). The SSM/I is a seven-channel radiometer operating on vertical and horizontal polarization at 19.35, 37.0, 85.5 and 22.235 GHz. The total swath width is 1400 km with a ground-pixel spacing of 25 km for the lower (19 to 37 GHz) and 12.5 km for the high fre-

EGU

quency (85 GHz) channel. The measured brightness temperature depends on surface temperature (TS), effective atmospheric temperature (TE), near surface wind speed (W), near-surface wind direction (Φ), WVC, liquid water content (L) and atmospheric pressure (P). The algorithm used for operational retrievals from SSM/I has been de-
5 veloped by Wentz (1997). Parameters retrieved are W, WVC and L. The dependence on TS is considered to be weak above ocean surfaces for which climatological input data is used to account, for example, for ENSO. Therefore the retrievals are restricted to ocean surfaces only. TE is specified from an empirical correlation with V and TS derived from radiosonde observations and W and Φ are dependent parameters. The
10 rms accuracy of the modelled brightness temperature is estimated to be between 0.5 and 1 K and the rms on the retrieved WVC is estimated to be 0.12 cm with an bias of 0.6 mm. From a detailed analysis of SSM/I averaging kernels and response functions, Engelen and Stephens (1999) reveal that SSM/I is especially sensitive to the lower troposphere over ocean surfaces, which is important for the quality of the total column
15 WV product. SSM/I retrievals are not affected by clouds except those with heavy precipitation events. SSM/I data quality can, however, be affected by small islands within the range of the observed ground pixel and are significantly affected by ice-cover. In the operational product both instances are usually masked out, however, strong deviations from correlated measurements are nevertheless reported, for example, at high
20 altitudes, which are attributed to impact of ice-shields on the retrievals (Noël et al., 2004).

DMSP SSM/I data has been assimilated in the most recent ECMWF reanalysis data set (ERA-40) for the period between 1987 until 2001 (Gérard and Saunders, 1999). Previous data sets, like ERA-15, were relying on data from the TIROS Operational
25 Vertical Sounder (TOVS). It is important to note for the purpose of this paper that temperature values from the latter instrument have also been assimilated in the NCEP reanalysis data-set (NRA) except for regions between 20 north and 20 south due to rain contamination (Kistler et al., 2001). For the NRA data set no attempts have been made so far to assimilate products from the SSM/I instrument series.

Hydrological cycle of MATCH

R. Lang and
M. G. Lawrence

Title Page

Abstract | Introduction

Conclusions | References

Tables | Figures

|◄ | ►|

◄ | ►

Back | Close

Full Screen / Esc

Print Version

Interactive Discussion

EGU

2.4. NVAP

The NASA water VApor Project (NVAP) (Randel et al., 1996) is an effort to blend various WV products from ground based radio-stations with satellite based observations. A first data set was constructed for the years 1988–1992 on a 1 by 1° spatial resolution and has been extended in recent years until 1999, comprising observations from TOVS and SSM/I. NVAP provides 3 atmospheric layers of WV content until 1994 adding a 4th layer in 1995. Recently the Next Generation data set called NVAP-NG has been provided (http://eosweb.larc.nasa.gov/PRODOCS/nvap/table_nvap.html) using an improved SSM/I antenna pattern correction, an optimal estimation assimilation scheme for data from the Advanced Microwave Scanning Unit (AMSU-B) and SSM/T2 (Special Sensor Microwave Temperature-2), as well as adding Tropical Rainfall Measuring Mission (TRMM) Microwave Imager (TMI) and Advanced TOVS (ATOVS) WVC values to the data set. For NVAP-NG also the resolution has been improved to half a degree horizontally and 5 layers in the vertical (Vonder Haar et al., 2003).

NVAP therefore provides a so far unique global WV data set where different instruments are combined according to their strengths and limitations. Simpson et al. (2001) compared the NVAP data from 1988 to 1995 to TOPEX/POSEIDON microwave radiometer WVC retrievals (TMW) and ECMWF reanalysis fields. They found that NVAP was drier than TMW, which was in turn drier than ECMWF fields. It was determined that NVAP has sufficient relative accuracy for variability studies, although its absolute accuracy is uncertain. Engelen and Stephens (1999) found in their study of the detailed response functions of SSM/I and TOVS that TOVS is sensitive to the middle and upper part of the troposphere but relies, for the lower troposphere, heavily on a priori information. Due to this known problem in the quality of total column TOVS data (Stephens et al., 1994) TOVS is weighted low as compared to SSM/I and radiosonde data in the NVAP blending procedure. Significant TOVS contributions to the global data set can be expected over remote land region where no high quality radiosonde data is available (e.g. Africa and the tropical South America). However, comparisons between models

Title Page

Abstract | Introduction

Conclusions | References

Tables | Figures

◄ | ►►

◄ | ►

Back | Close

Full Screen / Esc

Print Version

Interactive Discussion

EGU

driven by reanalysis data as well as reanalysis data sets themselves and NVAP are not independent because most of the data sets employed in NVAP (SSM/I, TOVS and radiosondes) are also used for the reanalysis products of NCEP and ECMWF.

3. Precipitation measurements

The Global Precipitation Climatology Project (GPCP) provides global gridded precipitation estimates from raingauge and satellite observations on a 2.5 by 2.5° horizontal grid (GPCP-V1)(Huffman et al., 1997; Rudolf, 2001). The data set comprises data from geostationary and polar-orbiting satellite infrared histograms for convective precipitation between 40° north and 40° south, SSM/I 19 GHz radiances for large-sacle frontal precipitation over the ocean, SSM/I 85 GHz radiances for large-scale precipitation in the extra-tropical land and ocean region, estimates from TOVS at high latitudes and from a gridded analysis of raingauge stations from about 7000 geolocations over land surfaces. Data is available starting from 1979 and is updated on a near real time basis. The general GPCP blending approach for the data is the use of preferences for the regionally best data sources, no use of data believed to be unreliable, the stepwise adaption of estimates of low quality to the more reliable ones, and the use of corrected raingauge measurements (Huffman et al., 1995). Recently the improved fully global combined product (GPCP-V2) has been published (Huffman et al., 2001; Adler et al., 2003). The data-set archive also contains the individual input fields, a combined satellite estimate, and error estimates for each field.

GPCP precipitation amounts have been compared to the NCEP-NCAR Climate Prediction Center Merged Analysis of Precipitation (CMAP) (Xie and Arkin, 1997) in various studies (Gruber et al., 2000; Rudolf, 2001). It has to be noted that CMAP is not a completely independent source from the GPCP data-set as it relies also on SSM/I data and uses the gauge-network provided by GPCP. In addition CMAP uses also data from the MSU instrument, which has been adjusted to gauge data from island and coastal stations. Both data-sets, CMAP and GPCP, are frequently used and available online.

EGU

Differences between the two data sets can be as large as 6.5 mm per day, where GPCP shows more precipitation over high latitude oceans, and less for Indonesia and the tropical Pacific for a case study based on monthly averaged data of January 1999 (Rudolf, 2001).

4. The NCEP reanalysis data sets

The NCEP reanalysis (NRA) system described in detail by Kalnay et al. (1996) employs the NCEP global spectral model with 28 sigma vertical levels and a horizontal triangular truncation of 62 nodes, which relates to about 200 km. A 3-dimensional variational (3-D-Var) scheme for assimilation of observational data is employed in spectral space using the 6-h forecast results of the model as the initial guess values. This also means that in regions with little data for 'adjustment' the analysis can be heavily influenced by the model. Using different model versions in the standard analysis system can therefore lead to significant changes in the results and artificial climate jumps. To prevent this, NRA uses the forecast model operational in 1995 for their most recent reanalysis system. The reanalysis is reported to be essentially free of the inhomogeneities due to changes in model resolution and physics (Kistler et al., 2001).

NRA uses data from upper air rawinsonde observations of temperature, horizontal wind, and specific humidity, from TOVS vertical temperature soundings over ocean except between 20 north and 20 south due to rain contamination, and TOVS temperature soundings over land above 100 hPa. Cloud tracked winds are incorporated from geostationary satellites, together with aircraft observations of wind and temperature, land surface reports of surface pressure, and oceanic reports of surface pressure, temperature, horizontal wind and specific humidity (for details on the individual data set see Kistler et al., 2001). For the focus period of this paper starting 1995, all of the named observation sources had been available.

A large set of output parameters are delivered by the reanalysis, a good fraction of which has been calculated online (model predicted) and have not been based on

[ACPD](#)

4, 7917–7984, 2004

Hydrological cycle of MATCH

R. Lang and
M. G. Lawrence

[Title Page](#)

[Abstract](#) | [Introduction](#)

[Conclusions](#) | [References](#)

[Tables](#) | [Figures](#)

[◄◄](#) | [►►](#)

[◄](#) | [►](#)

[Back](#) | [Close](#)

[Full Screen / Esc](#)

[Print Version](#)

[Interactive Discussion](#)

[EGU](#)

observational data directly and are labelled "C" variables (here we adapt the notation by Kistler et al., 2001). Others rely to a significant portion on the initial guess forecast values and are labelled with "B". Those which are dominated by the observations are labelled "A". "A" variables are for example upper air temperature and wind fields, whereas all moisture variables and those near the surface are usually labelled "B". Evaporation and precipitation are "C" variables.

For the purpose of the study presented here, the focus is on those parameters of the hydrological cycle evaluated for both the NRA and MATCH model output, like WV, and precipitation. Even though the long term dynamics of the hydrological parameters in the reanalysis data is an important and interesting subject for climate studies, like, for example, the steadily growing stronger hydrological cycle since 1991, here we are focusing on the consistency between the various parameters of the hydrological cycle in the individual models and with respect to observations. For a detailed discussion of the long term trends we refer to Kistler et al. (2001).

NRA reanalysis output has also been compared to reanalysis values from the ECMWF 0 to 6 and 12 to 24 h forecast models (ERA-06 and ERA-24) (Stendel and Arpe, 1997). Stendel and Arpe (1997) showed that the global hydrological cycle and surface energy budget are in better balance in the 12–24 h ERA forecasts than in the 0–6 h ERA forecasts. ERA global latent heat fluxes are about 10% higher than those by NRA and therefore compare better with the corrected observations by Da Silva et al. (1994). They also compared NRA precipitation data with data from the GPCP climatology. Over land all reanalysis results exceed the independent estimates in the tropics, while NRA has the most precipitation near 60° north. NRA has too much precipitation over Russia and Canada in summer (Janowiak et al., 1998). Over the ocean ERA clearly has the most rainfall in the tropics, where the GPCP and CMAP disagree with each other by as much as one mm per day. In the mid-latitude oceanic storm tracks both GPCP and CMAP estimates exceed the NRA and ERA precipitation amounts. NRA shows a strong correlation of precipitation with tropical air-sea temperature differences and to a significantly lesser extent with sea surface temperatures (SST).

Hydrological cycle of MATCH

R. Lang and
M. G. Lawrence

EGU

Moisture is a generally poorly measured variable in comparison to winds and temperature and is therefore a prototypical "B" variable. To the best of our knowledge little has been done so far to evaluate the water vapor fields of reanalysis model output with independent sources. This may be partly due to the lack of WV measurements on global scale which are not already assimilated in the NRA or ERA model. Kistler et al. (2001) report that a comparison of relative humidity between NRA and ERA shows qualitative good agreement with, however, systematic differences in relative humidity of the order of 10%. These are large differences when compared to the interannual variability.

5. MATCH

The Model of Atmospheric Transport and Chemistry (MATCH) is an "semi-online" model, where the most basic meteorological parameters, apart from those of the hydrological cycle, come from weather center analysis or reanalysis data. The model has been described in detail by Rasch et al. (1997); Mahowald et al. (1997a,b); Lawrence et al. (1999). Here we use temperature, pressure, horizontal winds, surface wind stresses, latent and sensible heat flux from NRA, described before, for model calculations of the months January and August between 1996 and 1998. The runs are performed at a horizontal resolution of T63 (96 by 192 latitude-longitude grid) corresponding to the resolution of the NRA input fields provided by NCAR. The terrain following 28 vertical sigma layers employed by NRA have been adopted. The meteorological data is read in every 6 h and is linearly interpolated to model time steps in between. The model includes representations of resolved scale transport, convective transport, boundary layer transport, and scavenging and deposition of soluble gases and aerosols (Lawrence, 1996; Lawrence et al., 1999; von Kuhlmann et al., 2003a). In contrast to other CTMs, MATCH has the capability of simulating online all cloud processes such as cloud water and ice content, cloud fraction, fraction of water converted to rain and snow as well as evaporation of hydrometeors. Using the evapotranspiration

R. Lang and
M. G. Lawrence

at the surfaces from NRA, MATCH then calculates the full tropospheric hydrological cycle online. All these processes can therefore consistently be used in the aforementioned model processes. In diagnosed mode, calculating the full hydrological cycle, the model runs approximately 4 times faster than the Commmunity Climate Model (CCM)
5   of NCAR (Rasch et al., 1997).

For resolved transport of cloud water the model uses the flux-form semi-Lagrangian scheme called SPITFIRE (Rasch and Lawrence, 1998) with a correction for the surface-pressure mismatch between interpolated input and model data (for details, see Jöckel et al., 2001; von Kuhlmann et al., 2003a). For the parameterization of moist con-
10 vection MATCH uses two schemes successively. First, the deep penetrative convection scheme by Zhang and McFarlane (1995) is applied reducing convective available potential energy (CAPE) within the total column from the surface to the upper troposphere. Then, a local convective transport scheme by Hack (1994) is used to remove all remaining instabilities representing shallow convection and mid-level convection not
15 originating in the boundary layer. The sensitivity of MATCH to the NRA input data and the convection parameterization employed is described in Mahowald et al. (1997a,b).

The parameterization of cloud microphysics in MATCH follows the parameterization developed by Rasch and Kristjánsson (1998). The cloud fraction parameterization depends on relative humidity, vertical motion, static stability, and convective properties
20 and is based on the work by Slingo (1987). The convective cloud fraction is also proportional to the rate at which mass is detrained from the parameterized convective updrafts above 500 mb, and to the convective mass flux for the updraft core cloud fractions. Clouds are permitted at all tropospheric layers. The total mass of condensate within each gridbox is predicted for both liquid and ice clouds and the conversion from
25 condensate to precipitation uses a bulk microphysical model. Precipitation values are then in turn used to drive wet scavenging of soluble gases and aerosols. The scavenging parameterization has been developed and tested in Lawrence and Crutzen (1998); Lawrence et al. (1999); Crutzen and Lawrence (2000).

A detailed study of the distribution of MATCH modelled WV with respect to the output

of other GCMs or CTMs, and the distribution of precipitation and WV with respect to measurements using meteorological reanalysis input fields has not previously been carried out.

6. Results

In this section the key results of the comparisons between modelled WV and precipitation fields and measurements are presented, followed by a discussion of the implication of these results in Sect. 7.

6.1. GOME WV fields

Figure 4 shows the comparison between GOME WVC and radiosonde data from the operational weather center sonde network provided by ECMWF. The scatter plots compares data from August and January between 1996 and 2000. The data is taken from launch sites located within the area covered by one GOME ground pixel and with a temporal correlation of less than three hours and cloud covers below 15%. Temporal and spatial cloud-free correlations have predominantly been found over Indonesia and Europe with some additional stations over North America. The significant scatter of 0.4 cm is likely to a large part related to the problem in correlating a single sonde measurement to the large area of 40 by 320 km covered by the GOME instrument. In addition, the quality of the sonde data can vary significantly depending on the type of instruments used, on-site monitoring of measurements and the post measurement quality check of the data. Here, only data with more than four measurements per launch have been used. Apart from removing data with physically unrealistic numbers, no additional quality assurance techniques have been applied, which may cause a number of measurements to deviate significantly from the GOME measurements. However, quality assurance of radiosonde data is a very complex and difficult task required for climate change monitoring (Lanzante at al, 2003) but of less importance for relative

EGU

R. Lang and
M. G. Lawrence

Title Page

Abstract | Introduction

Conclusions | References

Tables | Figures

◄ | ►

◄ | ►

Back | Close

Full Screen / Esc

Print Version

Interactive Discussion

EGU

short time scale comparisons. The bias of the correlation is found to be below 2.5% with a correlation of 70%, both supporting the high credibility of GOME data over land surfaces.

Over ocean surfaces we compare GOME WVC data with spatially correlated grid-ded (0.5 by 0.5°) SSM/I data from SSM/I descending orbits of the F13 and F14 DMSP satellite platforms (see Sect. 2.3). Figure 5 shows the correlation for August 1996 to 2000 and January 1996 to 2000 (excluding January 1999 because of an instrumen-tal problem of GOME affecting the employed spectral region of the WV absorption) with a standard deviations smaller than 0.5 cm, which we attribute to the significant differences between the instruments' spatial resolution (25 km resolution for SSM/I as opposed to 40 by 320 km resolution for GOME) and the reduced sensitivity over ocean surfaces for the GOME instrument as compared to land surfaces. The bias of this comparison is smaller than 1%. This demonstrates the capability of GOME to achieve good accuracy in WVC also over ocean surfaces, however, associated with an aver-aged increase in the retrieval error due to the low reflectivity of the ocean surface and therefore an increased contribution of photons scattering above the surface.

Figure 6 shows the global distribution of the monthly mean retrieval error for August and January 1996 to 1998 as provided by the distribution matrix of the individual re-trievals and consisting of an estimate of the model-parameter error, the forward-model error and the retrieval noise contributions (for details on the error analysis, the im-pact of multiple scattering and aerosol loading on the retrieval, we refer to Lang et al., 2003). The forward model error contribution contains the impact of aerosol scattering and absorption on the retrieval for two reference maritime and rural aerosol scenarios employed in dependence of the observed geolocation. The error values delivered by the retrieval are therefore good estimates of an upper error bound. This is due to the fact that, especially for the rural aerosol case, the employed scenarios are more an exception than a standard. The figure shows that the error is smallest (below 0.1 cm) in the subsidence regions with relatively large WV content and little cloud cover, i.e., good statistics. For the strongest WV signals along the Inter Tropical Convergence

R. Lang and
M. G. Lawrence

Zone (ITCZ) but small number of measurements the error is around 0.25 cm. The error is largest (up to 0.5 cm) at high latitudes, where the WV absorption signal is weak both due to the low WV content (nearly three orders of magnitude lower at the poles as compared to the ITCZ) and due to large solar zenith angles (SZA). Large SZA correspond to large air masses traversed by the detected photons, which in turn lead to high contributions of multiple scattering out and into the light path, which is not explicitly accounted for by the retrieval model. Therefore we generally restrict the retrieval to latitudes within 70 to 80° of the equator. The number of measurements averaged over one month (three years) varies between 2 to 5 (6 to 15) measurements along the ITCZ and up to 15 (45) for the highest latitudes. The higher retrieval errors at high latitudes are partially compensated in the multi-year average by the better statistics in this regions due to overlapping satellite passes. The relative error varies between below 5% along the ITCZ and the subsidence region, 25% between 50 to 60° and 100% and more around 70° and above for the hemispheric winter. In the hemispheric summer the relative error at 70 degrees is around 25 to 50%.

Figure 7 shows monthly mean WVC values from GOME and NVAP together with their residual for August 1998. The general WV distribution pattern compares very well up to very small details. However, the difference plot (lower panel of Fig. 7) also clearly identifies regions with systematic differences in the distribution pattern. NVAP is significantly moist over mountain areas like the Andes and the Rocky Mountains, the Kongo basin in Central Africa, over Greenland and the Himalaya. GOME-SSP retrieves systematically lower values over the Amazon and much higher over the Sahel zone region. It also exhibits a moist bias over NH land masses when compared to NVAP for this time of the year.

Figure 8 presents the three-year average residuals for NVAP and SSM/I monthly mean values when compared to GOME-SSP retrievals. As compared to the single year results of Fig. 7 some of the patterns are significantly reduced, like the moist NVAP bias over Greenland, though most of the other features examined before, remain to be significant. Over ocean the three-year average residuals for the two reference data

sets SSM/I and NVAP look quite similar because NVAP relies predominantly on SSM/I data over ocean surfaces.

The impact of mountain areas on the total retrieved WVC is much stronger in the case of GOME observations than for the NVAP WVC product. Especially for strong transitions between low and high surfaces (like for the Andes) the relatively coarse resolution of the standard NVAP product smears out the WV distribution significantly. The generally high WVC content over the eastern equatorial Pacific is extended into Central South America for both products (even though weaker on the land side for GOME-SSP) but is significantly more disturbed by the mountain chains in the case of GOME-SSP. In contrast GOME-SSP WVC values seem to be unreasonably low over the Central Amazon region and too high over the Sahel region. The latter is due to the strong impact of sand storms and aerosol content in this part of Africa during this month, while the former is presumably due to an impact of the surface albedo on the retrieval in this specific area, which will be discussed in Sect. 7. GOME-SSP also exhibits a number of dry spots along the ITCZ and the Pacific warm pool regions, which are not visible in the NVAP product, most of which can be attributed to unsatisfactory removal of clouds and low measurement statistics as they are also visible in the three years averaged comparisons with SSM/I data.

6.2. Comparison to model results

Monthly averaged WVC distributions for August and January 1996 to 1998 have been modelled employing the MATCH CTM with driving meteorological input parameters from NRA, as has been described in Sects. 4 and 5 of this paper. MATCH data has been written out at 10:30 local time to achieve maximum temporal overlap with GOME data. For comparisons between model and measurements we will first compare the model results with the observations on a global scale including globally and zonally averaged comparisons and then focus on regional scales with two exemplifying regions, Europe and the Southern Asian/Indian Ocean region.

Figures 9 to 12 show the monthly averaged global and zonal WVC distribution as

Hydrological cycle of MATCH

R. Lang and
M. G. Lawrence

modelled by MATCH and NRA and as measured by GOME-SSP in January and August 1998 (Figs. 9 and 12), as well as for the three years average from 1996 to 1998 for both months (Figs. 10 to 12). It is very important to emphasize that for all comparisons presented here the cloud-mask derived from the GOME-SSP retrievals has also been

5 applied to the model values, including the zonally and globally averaged results. This has consequences for the accuracy of the presented absolute values. First, applying a cloud mask generally reduces the modelled mean WVC values by about 0.5 cm (10 to 15%) on a global average, as estimated from comparisons between the modelled values with and without the GOME cloud mask applied (see Table 1). Second, it also

10 influences the relative comparison between observation and model results because of an effect we hereafter will refer to as the "common-cloud-problem". Table 1 denotes an "artificial" model moistening effect by applying only the GOME cloud mask to the model. This is because pixels with cloud contamination are usually corresponding to high WVC amounts "relative" to surrounding clear-sky pixels. However, ground pix-

15 els identified as cloudy by the GOME measurement do not necessarily correspond to cloudy model pixels. As a consequence of applying only the measured GOME cloud mask to the model, this will generally lead to moister model results as compared to the measurement clear-sky scenario because the GOME cloud-mask will partly masked out model clear-sky pixel and leave cloudy model pixels (with relative high WVC) in

20 the analysis. The impact of the "common-cloud-problem" on the comparisons is shown by the results in Table 1 and can be quantified as an effect of about 0.3 cm (10%) when compared to applying only the GOME cloud mask to the model results. Table 1 also shows that for instances of hemispheric winter cloud masking may lead to an even higher hemispheric mean value as compared to the unmasked means. This is because

25 high latitudes with very low WVC (especially for hemispheric winter) see more cloud cover and are therefore masked out applying the GOME cloud mask. This effect is, however, small for the global mean values and for hemispheric summer.

Figures 9 to 11 show, that MATCH generally models the global WV distribution quite well, from the moist ITCZ regions to the dry polar regions. MATCH also resembles

R. Lang and
M. G. Lawrence

the overall shape of the moist and convective regions. However, significant differences between MATCH and GOME-SSP exist on regional scales and in the magnitude of the WVC distribution. MATCH is systematically lower than what has been observed over the Atlantic ITCZ and in the Pacific warm-pool region for both seasons (Figs. 9 and 10)

5 and the moist areas commonly extend more to the north and to the south. The most pronounced features evident occur in the Western Pacific convergence zone. Here, MATCH significantly overestimates the southern branch of the Western Pacific split ITCZ in August and exhibits a too broad and moist feature in January in the same region, when compared to GOME measurements. These features become less pro-

10 nounced when comparing to the three years averages including also the non-ENSO year 1996 (Fig. 10). GOME-SSP is generally drier than MATCH over the northern hemisphere (NH) landmasses of Canada, as well as wide parts of Russia and the southern hemisphere (SH) oceans for August (Figs. 9 and 10). However, this conclusion also holds for the comparison between GOME-SSP and NVAP in Fig. 8 and may

15 therefore additionally point to a low WVC bias of the GOME data in this region. We will discuss these features in detail in the following section. The low bias of GOME-SSP over the SH oceans as observed before in the intercomparisons to NVAP and SSM/I values (Fig. 8) is also visible for the MATCH comparisons. For January, Figs. 9 and 10 show that MATCH is generally high as compared to GOME-SSP for NH oceans,

20 whereas MATCH agrees generally quite well with what is observed by GOME over land, except for Central Africa and the aforementioned Central Amazon region, where GOME-SSP is drier than MATCH output.

The global WV distribution as given by NRA (Fig. 11) generally resembles what has been modelled by MATCH. The shape of the ITCZ is quite similar to the MATCH model

25 results for both seasons. For example, the strong southern branch of the Western Pacific split ITCZ and the high WV values over NH land masses are similar features leading to similar residual patterns for NRA and MATCH when compared to the GOME-SSP results. NRA ITCZ values are, however, generally higher than those computed by MATCH. Differences are evident for the Central Amazon and Western Pacific regions,

EGU

where MATCH is moist over the ocean and dry over land when compared to NRA.

MATCH is about 0.1 to 0.3 cm lower in the globally averaged WV content as GOME-SSP, NVAP and NRA for August and compares well with GOME-SSP (within 0.1 cm difference) and NVAP for January as indicated by the lower panels of Fig. 12. For
5 January, the shape of the zonal distribution of all four products compares very well, however, NVAP and NRA peak significantly higher around the ITCZ than GOME-SSP and MATCH. A different picture occurs for the August zonal mean distributions. Here, NVAP, and GOME-SSP compare very well in shape and absolute quantities. MATCH is systematically low for the season with high WV content in the NH and around the
10 ITCZ, but the shape of the zonal WV distribution of MATCH again resembles quite well the shape of the NRA zonally averaged values.

Figure 13 (upper panels) shows averaged daily PR as given by GPCP (cf. Sect. 3) for August (left panels) and January (right panels) 1996 to 1998. The middle panels of Fig. 13 show the corresponding model results from MATCH. MATCH models the
15 basic patterns very well, like the continuous stream of precipitation along 10° north in August and the more distinct precipitation fields over the south western Pacific, Central South America, Africa and the Pacific Warm Pool. Differences occur, similar to the WVC distributions, on regional scales and due to differences in the absolute values (lower panel of Fig. 13). MATCH PR are weaker along the ITCZ and more spread out
20 in latitude leading to significant residuals of high MATCH PR north and southwards of the ITCZ (e.g., the overestimation in precipitation along the southern branch of the Western Pacific split ITCZ in August). MATCH models significantly higher PR over the Central South American and Central African land masses for January and over North America, Europe and Russia for August, as compared to what has been measured by
25 the GPCP observations.

As MATCH is driven by NRA parameters like temperature, wind fields, and evapo-transpiration rates, with potentially significant influence on the modelled WV and pre-cipitation patterns, the comparisons presented in Fig. 14 give an indication to which extent MATCH precipitation model output may depend on NRA input parameters. The

Hydrological cycle of MATCH

R. Lang and
M. G. Lawrence

Title Page

Abstract	Introduction
Conclusions	References
Tables	Figures

◄◄   ►►

◄   ►

Back   Close

Full Screen / Esc

Print Version

Interactive Discussion

EGU

Hydrological cycle of MATCH

R. Lang and
M. G. Lawrence

figure compares NRA PR to those given by GPCP in a similar fashion as the comparisons presented in Fig. 13. The NRA precipitation distribution is for large parts of the globe closely related to the MATCH modelled PR indicating the strong influence of the before mentioned shared parameters on the precipitation distributions modelled

5 by both products. The residual patterns of Fig. 14, however, also reveal significant regional differences to what has been modelled by MATCH. MATCH PR are generally higher over NH land masses in August and over the Central Amazon and Central African regions for January. There are considerably less differences in the precipitation residuals for NRA and MATCH over ocean surfaces. Generally the residuals of Figs. 13

10 and 14 differ predominantly in magnitude and less in shape and geolocation.

Figure 15 additionally provides the MATCH modelled contribution of convective to the total (large-scale plus convective) amount of precipitation, showing that seasonal changes in the residual patterns of Figs. 13 and 14 are frequently related to changes in the relative contribution of convective precipitation. Generally, the large model to

15 observation residuals correspond to the shift between north and south in the convective precipitation for hemispheric summer.

Figures 16 and 17 provide a more detailed look at regional differences between model and measurements for Europe and the Indian Ocean/Southeast Asian region. Residuals between model and observations for WVC (upper panels) and PR (lower

20 panels) distributions are given for the three-year averages of August 1996 to 1998, i.e. for the summer season. MATCH and NRA show high atmospheric WV content over European land masses in August and low biases over the Mediterranean ocean and North Africa (Fig. 16). The close relation between NRA and MATCH WVC distribution, as has been observed before for the global comparisons, is evident from Fig. 16.

25 MATCH is, however, generally drier than NRA but exhibits, in turn, higher PR. NRA and MATCH show similar residual patterns in precipitation with an emphasize on regions with high elevations. The Indian Ocean/Southeast Asian region (Fig. 17) exhibits similar relations between WV and precipitation residual patterns. Regions with relatively high WV content as compared to the GOME measurements, over land and south of

EGU

the Equator, correspond to regions with high PR when compared to the GPCP measurements and vice versa. A detailed discussion of the observed relation between WV and precipitation patterns is given in the following discussion section.

The comparisons presented here are finally summarized in Table 2 which presents the global and regional mean values in WVC content, PR and WV residence time. The latter has been calculated as the ratio between WVC and PR and serves as an useful measure for the modelled and observed mean conversion of WV into precipitation, as discussed further in the following section.

7. Discussion

There are four immediate qualitative conclusions which can be drawn from the above comparisons: First, GOME compares well to independent measurements of WVC by SSM/I over oceans and reasonably to measurements compiled by NVAP over land. Second, MATCH models the general global PR and atmospheric WV content quite well with a tendency to be on average drier than the observations and the reanalysis data. Third, the WV distribution patterns as modelled by MATCH are quite similar to those given by NRA, whereas both MATCH and NRA exhibit significant regional differences to what has been observed by GOME. Fourth, the WVC residuals between MATCH and the GOME observations are for wide parts of the globe similar to residuals observed in the PR between MATCH model results and GPCP observations. These main points are discussed in detail in this section.

7.1. GOME observations

From comparisons between GOME WVC distributions and those given by other observation products, like SSM/I and NVAP (Fig. 8), GOME-SSP data quality over the Central Amazonian rain forest region and the African Sahel zone may be doubtful. Especially in the latter case, GOME exhibits some unusually high column values at around $15°$

north of the equator for August 1998, which might be related to the impact of Saharan dust and an increased contribution of multiple scattering, which is not accounted for by the retrieval method. Comparisons with radiosonde measurements (not shown) also reveal some extraordinary high GOME WVC measurements in this region. GOME-SSP

5 WV columns are systematically lower than what has been observed by NVAP and what is given by NRA over the Central Amazon and Central African region especially for the high WV content periods in January. Here, the surface albedo around the 590 nm retrieval window is a matter of concern, because the retrieval assumes a linear behavior of the albedo over the spectral region applied, which is usually not the case for predom-

10 inantly green surfaces in this region of the spectrum. However, NVAP and NRA both rely predominantly on TOVS data over remote land regions and for the investigated periods, which is known, in turn, to heavily rely on a priori climatology information for the lower part of the atmosphere and therefore also for the total column values (cf. 2.4 and references therein). The latter might also be the reason why NVAP and NRA ex-

15 hibit high WVC when compared to GOME over various land surfaces, especially over Canada, and wide parts of Russia (Siberia) and China in August.

The ITCZ land regions must be labelled to be the most critical for drawing ridged conclusions from the presented comparisons. These regions are usually also very sparse in radiosonde measurements and data-quality for NVAP and NRA data is therefore

20 low. In addition, regions of the ITCZ are predominantly covered by clouds, which leads to an significantly reduced statistics and increased biases in the GOME data, as well as to an increased impact of residual cloud contamination on the retrieved WVC from GOME. Similar conclusions hold for GOME-SSP WVC measurements along the ITCZ over ocean surfaces. But, in this case and in contrast to land regions, the quality

25 of GOME-SSP data can be estimated more rigorously by comparison to high quality SSM/I measurements available for this region. GOME shows smaller averaged WVCs along the ITCZ as compared to SSM/I by up to 0.5 cm, for specific regions as much as 1 cm (e.g. the Pacific warm pool) on a three years average, and predominantly related to residual cloud contamination of the observed scene. However, due to the differences

Hydrological cycle of MATCH

R. Lang and
M. G. Lawrence

Title Page

Abstract | Introduction

Conclusions | References

Tables | Figures

◄ | ►

◄ | ►

Back | Close

Full Screen / Esc

Print Version

Interactive Discussion

EGU

in surface albedo between land and ocean surfaces, this result cannot be used as an estimate for GOME-SSP biases over ITCZ land regions. Cloud statistics and residual cloud contamination lead to significantly smaller zonally averaged GOME-SSP values around the ITCZ (up to 0.6 cm) as compared to NVAP and NRA. This effect is then
⁵ consequently also visible in the globally averaged WVC values (Fig. 12).

GOME-SSP tends to deliver smaller WVC as observed by NVAP and SSM/I for the SH oceans for August 1996 to 1998 and NH oceans in January (Fig. 8). On a zonal average (Fig. 12) the effect is small for NH summer (less than 0.2 cm) but becomes significant for NH winter (more than 0.4 cm). This bias is probably due to the impact
¹⁰ of hygroscopic aerosols (like, for example, sea salt), which grow significantly under low relative humidity conditions forming haze and thin cloud layers.

7.2. Distribution of WV and precipitation

It is beyond the scope of this paper to analyze the detailed mechanisms behind the observed differences between MATCH and the observations but the results presented
¹⁵ here encourage us to make those mechanisms subject of a follow-up study. Here, we focus on the question: where are significant differences between MATCH and the observations found and which of those are unique to the MATCH model and therefore missing in a comparison between GOME-SSP data to NRA data. We call the observed differences significant for residual patterns, which are well outside the range of the
²⁰ 1-σ measurement and method of comparison related errors as discussed before (cf. Sects. 2.1 to 5, and Figs. 5 to 8). GOME-SSP retrieval biases have been estimated to range between less than 0.1 cm (subsidence regions) and up to 0.6 cm (hemispheric oceans in winter and ITCZ region).

Along the ITCZ region MATCH is significantly drier than NRA, but exhibits generally
²⁵ very similar patterns with respect to the reanalysis values in the global WV distribution, as well as in the latitudinal dependence of the zonally averaged values for both seasons. This is not surprising because MATCH and NRA share two of the most important parameters determining the amount of atmospheric WV content: temperature and the

rate of evapotranspiration. In addition, the distribution patterns of WV are significantly influenced by transport processes (and therefore by the wind-fields delivered by NRA), due to the relatively long residence time (the global mean WV content divided by the global mean PR per day) of WV of on average 6 days (1996 to 1998). Differences

5 between NRA and MATCH WV and precipitation fields can therefore be attributed to differences between NRA and MATCH in the modelled production of cloud and precipitation, as well as the parameterization of the re-evaporation of hydrometeors. For example, an inefficient re-evaporation of hydrometeors in the modelled precipitation columns would lead to a too dry model with decreasing WV residence time because of

10 increasing precipitation and vice versa.

Figures 13 and 14 show a comparison between MATCH and NRA modelled precipitation (note that precipitation in NRA is a "C"-variable and not assimilated from measurements but calculated "online") to the observations as given by GPCP confirming the strong influence of shared parameters (see also previous section) leading to the

15 strong similarity in the general precipitation patterns between both models. A comparison between the residual panels of Figs. 13 and 14 (lower panels) identifies a number of regions, especially over the oceans, where NRA shows similar residuals in precipitation with respect to the observations than MATCH. MATCH precipitation patterns along the ITCZ but also along NH land masses, Canada, the eastern part of the U.S., as well

20 as Europe and Russia are therefore expected to be significantly influenced by NRA. In contrast, other regions can be identified, like the Central Amazonian and Central Africa, where MATCH exhibits stronger residual patterns than NRA. Those areas may be attributed as regions where specific MATCH parameterizations of the hydrological cycle may significantly contribute to the observed differences. Local residuals between the

25 modelled precipitation patterns and the measurements we call significant for difference values larger than 0.3 cm per day in view of error estimates given by GPCP (Sect. 3).

Figure 15 shows the relative contribution of convective to the total (large-scale plus convective) amount of precipitation as has been modelled by MATCH. From a comparison between Figs. 13 to 15 we conclude that differences in the residuals to the

EGU

observations between MATCH and NRA are often correlated with regions of dominant contribution of convective precipitation. For example, strong differences over Central Africa and Central Amazonian exist especially for SH summer correlated to the position of the ITCZ with strong convective updrafts. The differences in the precipitation between MATCH and GPCP over western Canada and Siberia are also evident solely for NH summer, where these regions see significant contribution of convective precipitation. The subsiding regions north and south of the ITCZ are dominated by residual patterns which are common to both MATCH and NRA comparisons to observations. Here the employed NRA evapotranspiration rates in MATCH should be of our main concern. As has been discussed in Sect. 4, errors in the modelled evapotranspiration rate (evapotranspiration is a "C"-variable derived from vapor pressure, surface temperature, the net irradiation flux, and wind speed, some of which are labelled as poorly measured "B"-variables) serve as the dominant source of errors for differences between modelled and observed PR over longer time scales (Kistler et al., 2001; Stendel and Arpe, 1997).

7.3.   Correlations between WV and precipitation residuals

Figures 16 and 17 relate residual patterns between MATCH and NRA modelled and observed quantities for WV and precipitation for August 1996 to 1998. Figure 16 focuses on Europe, where an overestimation of precipitation by MATCH and NRA with respect to GPCP observations is regionally correlated to an overestimation in the modelled WV content when compared to the GOME results. The differences occur mainly over land. August sees generally a high contribution of convective precipitation over European land masses (cf. Fig. 15). Besides the higher WVC of NRA compared with GOME-SSP over land, NRA precipitation amounts are on average lower over Europe than those modelled by MATCH and come closer to what has been observed by GPCP (see Table 2). This indicates that specific MATCH parameterizations, presumably related to convective updrafts, produce more precipitate than NRA and with respect to the observations. We also note the close relationship in WV residual pattern between the

EGU

Hydrological cycle of MATCH

R. Lang and
M. G. Lawrence

NRA and MATCH model comparisons to GOME observations. A possible source may be an overestimated WV input by high evapotranspiration rates, which are common to both MATCH and NRA. The generally drier MATCH model as compared to NRA may then be explained by an ineffecient re-evaporation of precipitate in the MATCH model

5 leading also to the higher observed precipitation amounts as compared to NRA. In contrast, a general bias in the GOME-SSP data (too dry over land and too moist over the Mediterranean and North Africa) may also explain the observed differences. However, GOME-SSP comparisons with the European radiosonde network show only very small biases below 3% and comparison with SSM/I data over the Mediterranean re-

10 gion confirm a higher WV content as has been modelled by MATCH and NRA over this region (see Fig. 8). The elevation signal visible in both, the NRA and the MATCH WV residual patterns, may also point to problems in comparing the coarse latitudinal model resolution (about 1.8°) to the relatively high latitudinal resolutions of the GOME measurements (about 0.4°). But close relations between WV and precipitation resid-

15 ual patterns as examined, for example, above the Alps, the Carpatians, Scandinavia and the Kaukasus mountains, leads us to question the models performance in regions with orographically induced convection. Additionally, other European land regions (e.g., Germany, Poland, and Russia) also show close relationships between WV and precipitation residual patterns.

20 The global atmospheric WV content is predominantly constrained by temperature via the Clausius Clapeyron relationship, providing that the relative humidity stays approximately constant. Precipitation is then closely linked to the evapotranspiration rate. However, this relationship only holds for large scale averages, not influenced by the local to regional weather dynamics, the regional net incoming radiation, or differences

25 in surface types and soil moister content. The observed positive correlations of precipitation to WV residual patterns may therefore be attributed to regional increases in PR through a regional increased availability of WV for both NRA and MATCH and over European land masses. In addition, MATCH exhibits a too rapid conversion of WV into precipitate when compared to NRA. The high WV content over land may in turn be at-

tributed to too high evapotranspiration rates in the case of MATCH and NRA, and likely additional biases in NRA output by assimilation of TOVS lower tropospheric data over land, which in turn heavily relies on a priori model data and may therefore lead to the observed stronger WV bias of NRA when compared to MATCH data.

5 High WVC over European land masses for NRA and MATCH are balanced by low WVC over the Mediterranean and North Africa, in the sense that the mean WV content of NRA and MATCH comes close to what has been observed by GOME-SSP over the entire region (see Table 2). However, the MATCH WV residence time is significantly lower than given by NRA and the GOME-SSP and GPCP observations. This

10 is because of the on average higher PR of MATCH when compared to the latter. Table 2 shows that this also holds for the global mean values, for which MATCH appears to model about one day shorter residence times because of the higher mean precipitation-rate values.

Figure 17 confirms the strong regional close relation between WV and precipita-

15 tion residual patterns as has been observed before for Europe, but now for the Indian Ocean/Southeast Asian ITCZ region for August 1996 to 1998. Again, MATCH PR are on average significantly higher than what has been observed. However, in this region, the differences between NRA and MATCH in mean PR are small for both August and January (cf. Table 2), but, because MATCH is generally drier along the ITCZ regions,

20 the MATCH modelled residence time is again lower when compared to NRA and the observations. Table 2 also shows that MATCH modelled residence time for Europe and the Indian Ocean compare much better to what has been observed and to what has been provided by NRA in January. For NH winter the contribution of convective precipitation to the total is small or negligible over Europe, and weakened for the observed

25 Indian Ocean region. This additionally confirms the link between MATCH residuals in both WV and precipitation with regions of strong convection.

We want to add here, that both models, NRA and MATCH, lack a detailed cloud-microphysical scheme. This has numerous consequences and may partly explain observed differences to observation for both data-sets, for example, in regions with high

Hydrological cycle of MATCH

R. Lang and
M. G. Lawrence

EGU

aerosol loading as above Central Europe, India, China and Indonesia. A detailed analysis of the impact on cloud micro-physics on the results, however, requires significantly improved observational data sets (especially with respect to spatial resolution), as well as detailed regional studies comprising additional sets of modelled and observed optical parameters (Feichter et al., 2004). This would be valuable to examine in future studies. However, in order to be able to perform a successful study on the consequences of new parameterizations in cloud microphysics and its effect on modelling the hydrological cycle, the impact of the applied meteorological re-analysis data-sets and the employed cloud parameterizations on the current model results, as has been laid out in this study, has to be estimated in detail together with the underlying mechanisms leading to differences between model output and observations, which will be subject of a subsequent study to what is presented here.

8. Summary

The main objective of this study was to answer the question how well key parameters of the hydrological cycle like WV and precipitation are represented by the semi-offline model MATCH driven by NRA and to identify regions with potential problems in the MATCH parameterizations related to the formation of cloud and precipitation, as well as regions with potential deficiencies in the employed reanalysis data. The results of this study may therefore be of use in subsequent model sensitivity studies employing and testing different convective cloud model parameterizations, different reanalysis data sets (e.g., ERA reanalysis instead of NRA), as well as new cloud micro-physical schemes for use in CTMs and GCMs. An additional objective of the paper is to demonstrate the capabilities of the GOME WV data record to be used for model evaluations on global and regional scales and as a truly independent source with respect to the reanalysis data-sets.

The GOME instrument provides a database from 1995 to the present over all surface types, whereas most other instruments measuring WV with a comparable record

R. Lang and
M. G. Lawrence

of data are restricted to either land or ocean surfaces. However, GOME retrievals are performed employing a WV absorption around 590 nm, which is affected by cloud contamination of the line-of-sight. GOME-SSP retrieved differences to other independent measurement sources, like those from the SSM/I instrument over oceans and the

5   NVAP blended WV database over ocean and land, are generally significantly lower than 0.5 cm except for regions along the ITCZ, where frequent occurrence of cloud contaminated ground pixels introduces differences up to 1 cm in the three years averaged monthly WVC. The study showed that some remote land regions like the Central Amazon and Central Africa exhibit significant residuals (between 0.5 and 1 cm)

10   when compared to NVAP. One possible explanation is that the influence of ground albedo (Central Amazon) and aerosol scattering (Sahel zone) lead to defective WVC retrievals. The impact of hygroscopic aerosols (like sea salt) under high relative humidity condition probably leads to the observed dry bias of the GOME-SSP retrievals for hemispheric winter over ocean surfaces. We concluded that the possible influence

15   of green surfaces on the retrieval should be evaluated by employing the SSP retrieval method to other WV absorption bands contained in the GOME spectrum (around 640 or 720 nm). The impact of large hygroscopic aerosols on the retrieval may be studied employing recent newly developed aerosol modules in model calculations with simple relationships between aerosol mass relative humidity and aerosol optical properties

20   (Metzger et al., 2002). Such studies are currently underway along with employing improved temperature and pressure profiles from reanalysis data for the calculation of reference absorption line-parameters in SSP.

MATCH calculates both WV and precipitation fields online, whereas for the NRA data set only precipitation amounts are online modelled quantities and not directly forced by

25   measurements. The shape of the MATCH modelled zonally averaged WV closely resembles the shape of the zonally averaged NRA data set, because the MATCH version employed here uses parameters essential for modelling the hydrological cycle, like temperature, wind fields and latent heat fluxes, from NRA. However regional differences in the WVC distributions have been identified. MATCH is significantly drier along the ITCZ

than NRA for both seasons and moderately dry compared to the GOME-SSP observations in August. MATCH appears to have problems in modelling the WV content in regions of strong upward convection like along the ITCZ. As a consequence of the relatively dry convergence zone regions, MATCH is globally drier by about 0.2 cm than the NRA data set. GOME-SSP is also biased dry along the ITCZ through reduced monthly WVC statistics and residual cloud contamination. Therefore, GOME-SSP global mean WVC values are comparable to MATCH global mean values especially for January where the ITCZ regions are predominantly oceanic with longer cloud lifetimes. GOME-SSP derived global mean WVC are therefore generally smaller than those provided by NRA.

Regional differences between MATCH modelled WV columns and the observations can be as large as 2 cm on the basis of a three years monthly average. This conclusion also holds for differences observed between GOME-SSP and NRA data, whereas the NRA and MATCH WV distribution patterns generally closely resemble each other. MATCH and NRA share significant common WVC residuals to the GOME-SSP observations over NH land masses, especially Canada and the U.S. East Coast, over Europe and wide parts of Russia for August, and over Central Africa and South America for January. There are also a number of oceanic regions along the ITCZ, like the southern branch of the Eastern Pacific split ITCZ for both seasons and the Indian Ocean region along the equator in August showing high WVC when compared to GOME observations. NRA WVC residuals are generally larger than those observed from the MATCH comparisons to the observations. One possible conclusion that might be drawn from the comparisons is that a deficiency in the modelled evapotranspiration rates and the assimilated TOVS WV data leads to too high or too low WVC over the mentioned regions.

This conclusion is further supported by the fact that regions of high WVC are generally closely related to regions of too high model PR and vice versa for both MATCH and NRA output. The latter has been evaluated from a set of PR observations comprised in the GPCP data set. This similarity in WV and precipitation patterns have been

observed on a global scale, as well as over Europe and the Indian Ocean/Southeast Asian region. Even though GOME-SSP exhibits only small biases when compared to accurate data sets like SSM/I and radiosondes, and except for the instances mentioned before, it should be noted here that it might nevertheless be possible that the observed
5 common biases in the presented comparisons might partly be due to biases in the GOME observations. Regions like remote hemispheric land masses should therefore be subject of further evaluation of the quality of GOME retrieved WVC in additional studies.

    MATCH generally exhibits too high mean PR when compared to both GPCP obser-
10 vations and NRA output. This study therefore suggests that a too rapid conversion of WV to precipitate in MATCH, especially in instances of strong convection, leads to regionally too dry model results and in turn to generally too low WV residence times when compared to regional and global mean values from NRA, and GOME-SSP and GPCP observations.

15 In summary we therefore conclude that a study on the usage of a different or improved set of reanalysis data to drive the MATCH model is required to examine the impact on the modelled WVC distribution. In addition, the re-examination of MATCH cloud formation and precipitation parameterizations for strong convective events is also required in order to improve MATCH modelled precipitation fields. These results will be
20 of relevance especially with respect to the regional to global scale impact of anthropogenic emissions on weather and climate via the strong link between the hydrological cycle and the atmospheric HO_x chemistry, wet scavenging of aerosols and trace gases and it will be of major importance for present sensitivity model sensitivity studies using MATCH employing and testing new sets of aerosol model parameterizations.

Hydrological cycle of MATCH

R. Lang and
M. G. Lawrence

Print Version

Interactive Discussion

EGU

References

Adler, R. F., Huffman, G. J., Chang, A., Ferraro, R., Xie, P. P., Janowiak, J., Rudolf, B., Schneider, U., Curtis, S., Bolvin, D., Gruber, A., Susskind, J., Arkin, P., and Nelkin, E.: The version-2 global precipitation climatology project (GPCP) monthly precipitation analysis (1979–present), J. Hydrometeor, 4, 6, 1147–1167, 2003. 7930

Albert, P., Bennartz, R., and Fischer, J.: Remote Sensing of Atmospheric Water Vapor from Backscattered Sunlight in Cloudy Atmospheres, J. Atmos. Ocean. Tech., 18, 865–874, 2001. 7925

Bonn, B., von Kuhlmann, R., and Lawrence, M. G.: High contribution of biogenic hydroperoxides to secondary organic aerosol formation, Geophys. Res. Lett., 31, 10, L10108, doi:10.1029/2003GL019172, 2004. 7920

Burrows, J. P., Weber, M., Buchwitz, M., Rozanov, V., Ladstätter-Weienmayer, A., Richter, A., deBeek, R., Hoogen, R., Bramstedt, K., Eichmann, K.-U., and Eisinger, M.: The Global Ozone Monitoring Experiment (GOME): Mission Concept and First Scientific Results, J. Atmos. Sci., 56, 151–175, 1999. 7923

Casadio, S., Zehner, C., Piscane, G., and Putz, E.: Empirical Retrieval of Atmospheric Air Mass Factor (ERA) for the Measurement of Water Vapor Vertical Content using GOME Data, Geophys. Res. Lett., 27, 1483–1486, 2000. 7924

Crutzen, P. J. and Lawrence, M. G.: The Impact of Precipitation Scavenging on the Transport of Trace Gases: A 3-Dimensional Model Sensitivity Study, J. Atmos. Chem., 37, 81–112, 2000. 7934

Da Silva, A., Young, C. C., and Levitus, S.: Atlas of Surface Marine Data 1994 Vol. I: Algorithms

EGU

and Procedures, NOAA Atlas NESDIS 6, U.S. Dept. Of Commerce, Washington, D.C., 83 pp, 1994. 7932

Engelen, R. J. and Stephens, G. L.: Characterization of water-vapor retrievals from TOVS/HIRS and SSM/T-2 measurments, Q. J. R. Meteorol. Soc., 125, 331–351, 1999. 7921, 7928, 7929

5 ESA: The Global Ozone Monitoring Experiment Users Manual, edited by: Bednarz, F., ESA Publication SP-1182, ESA Publication Division, ESTEC, Noordwijk, The Netherlands, 1995. 7923

Feichter, J., Roeckner, E., Lohmann, U., and Liepert, B.: Nonlinear aspects of the climate response to greenhouse gas and aerosol forcing, J. Climate, 17, 12, 2384–2398, 2004.
10 7950

Gérard, É. and Saunders, R. W.: Four-dimensional variational assimilation os Spectral Sensor microwave/Imager total column water vapour in the ECMWF model, Q. J. R. Meteorol. Soc., 125, 3077–3101, 1999. 7928

Gruber, A., Su, X. J., Kanamitsu, M., and Schemm, J.: The comparison of two merged rain
15 gauge-satellite precipitation datasets, Bull. Americ. Meteorol. Soc., 81, 11, 2631–2644, 2000. 7930

Grzegorski, M.: Bestimmung von Wolkenparametern für das Global Ozone Monitoring Experiment mit breitbandigen Spektrometern und aus Absorptionsbanden von Sauerstoffdimeren, diploma thesis, Institute for Environmental Physics, University Heidelberg, 2003. 7927

20 Hack, J. J.: Parameterization of moist convection in the National Center for Atmospheric research community climate model (CCM2), J. Geophys. Res., 99, 5551–5568, 1994. 7934

Hollinger, J., Pierce, J., Lo, R., and Poe, G.: SSM/I instrument evaluation, IEEE Trans. Geosci. Remote Sensing, 28, 781–790, 1990. 7927

Huffman, G. J., Adler, R. F., Rudolf, B., Schneider, U., and Keehn, P. R.: Global precipitation
25 estimates based on a technique for combining satellite-based estimates, raingauge analyses and NWP model information, J. Climate, 8, 5, 1284–1295, 1995. 7930

Huffman, G. J., Adler, R. F., Arkin, P. A., Chang, A., Ferraro, R., Gruber, A., Janowiak, J., McNab, A., Rudolf, B., and Schneider, U.: The global precipitation climatology project (GPCP) combined precipitation dataset, Bull. Americ. Meteorol. Soc., 78, 1, 5–20, 1997. 7930

30 Huffman, G. J., Adler, R. F., Morrissey, M. M., Bolvin, D. T., Curtis, S., Joyce, R., McGavock, B., and Susskind, J.: Global precipitation at one-degree daily resolution from multisatellite observations, J. Hydrometeor., 2, 1, 36–50, 2001. 7930

Jöckel, P., von Kuhlmann, R., Lawrence, M. G., Steil, B., Brenninkmeijer, C. A. M., Crutzen,

Title Page

Abstract	Introduction
Conclusions	References
Tables	Figures

|◄ | ►|

◄ | ►

Back | Close

Full Screen / Esc

Print Version

Interactive Discussion

EGU

P. J., Rasch, P. J., and Eaton, B.: On a fundamental problem in implementing flux-form advection schemes for tracer transport in 3-dimensional general circulation and chemistry transport models, Q. J. R. Meteorol. Soc., 127, 1035–1052, 2001. 7934

Janowiak, J. E., Gruber, A., Kondragunta, C. R., Livezey, R. E., and Huffman, G. J.: A comparison of the NCEP/NCAR reanalysis precipitation and the GPCP raingauge-satellite combined data set with observational error considerations, J. Climate, 11, 2960–2979, 1998. 7932

Jones, P. D.: Recent Warming in global temperature series, Geophys. Res. Lett., 21, 1149–1152, 1994.

Kalnay, E., Kanamitsu, M., Kistler, R., Collins, W., Deaven, D., Gandin, L., Iredell, M., Saha, S., White, G., Woollen, J., Zhu, Y., Chelliah, M., Ebisuzaki, W., Higgins, W., Janowiak, J., Mo, K. C., Ropelewski, C., Wang, J., Leetmaa, A., Reynolds, R., Jenne, R., and Joseph, D.: The NCEP/NCAR 40-year reanalysis project, Bull. Americ. Meteorol. Soc., 77, 3, 437–471, 1996. 7931

Kistler, R., Kalnay, E., Collins, W., Saha, S., White, G., Woollen, J., Chelliah, M., Ebisuzaki, W., Kanamitsu, M., Kousky, V., van den Dool, H., Jenne, R., and Fiorino, M.: The NCEP-NCAR 50-year reanalysis: Monthly means CD-ROM and documentation, Bull. Americ. Meteorol. Soc., 82, 2, 247–267, 2001. 7928, 7931, 7932, 7933, 7947

Koster, R. D., Dirmeyer, P. A., Guo, Z., Bonan, G., Chan, E., Cox, P., Gordon, C. T., Kanae, S., Kowalczyk, E., Lawrence, D., Liu, P., Lu, C.-H., Malyshev, S., McAvaney, B., Mitchell, K., Mocko, D., Oki, T., Oleson, K., Pitman, A., Sud, Y. C., Taylor, C. M., Verseghy, D., Vasic, R., Xue, Y., and Yamada, T.: Regions of Strong Coupling Between Soil Moisture and Precipitation, Science, 305, 1138–1140, 2004.

Koelemeijer, R. B. A., Stammes, P., and Stam, D.: Spectral Surface Albedo Derived From GOME Data, Proc. 3rd ERS Symp. on Space at the service of our Enviroment, Florence, Italy, 17–21 March 1997, ESA SP-414, 3 Vols, 1997. 7926

Koelemeijer, R. B. A., Stammes, P., Hovenier, J. W., and de Haan, J. F.: A fast method for retrieval of cloud parameters using oxygen A band measurements from the Global Ozone Monitoring Experiment, J. Geophys. Res., 106, D4, 3475–3490, 2001. 7926

Kunhikrishnan, T., Lawrence, M. G., von Kuhlmann, R., Richter, A., Ladstätter-Weißenmayer, A., and Burrows, J. P.: Analysis of tropospheric NO$_x$ over Asia using the Model of Atmopsheric Transport and Chemsitry (MATCH-MPIC) and GOME satellite observations, Atmos. Envir., 38, 581–596, 2004a. 7920

Kunhikrishnan, T., Lawrence, M. G., and von Kuhlmann, R.: Semiannual NO$_2$ plumes during the

monsoon transition periods over the central Indian Ocean, Geophys. Res. Lett., 31, L08110, doi:10.1029/2003GL019269, 2004b. 7920

Kunhikrishnan, T. and Lawrence, M. G.: Sensitivity of NO_x over the Indian Ocean top emissions from the surrounding continents and nonlinearities in atmospheric chemistry responses, Geophys. Res. Lett., 31, doi:10.1029/2004GL020210, 2004c. 7920

Labrador, L. J., von Kuhlmann, R., and Lawrence, M. G.: Strong sensitivity of the global mean OH concentration and the tropospheric oxidizing efficiency to the source of NO_x from lightning, Geophys. Res. Lett., 31, 6, L06102, doi:10.1029/2003GL019229, 2004a. 7920

Labrador, L. J., von Kuhlmann, R., and Lawrence, M. G.: The effects of lightning-produced NO_x and its vertical distribution on atmopsheric chemistry: sensitivity simulations with MATCH-MPIC, Atmos. Chem. Phys. Discuss., 4, 6239–6281, 2004b,
SRef-ID: 1680-7375/acpd/2004-4-6239. 7920

Lang, R., Maurellis, A. N., van der Zande, W. J., Aben, I., Landgraf, J., and Ubachs, W.: Forward Modeling and Retrieval of Water Vapor from GOME: Treatment of Narrow Band Absorption Spectra, J. Geophys. Res., 107, D16, doi:10.1029/2001JD001453, 2002. 7924

Lang, R., Williams, J. E., Maurellis, A. N., and van der Zande, W. J.: Application of the Spectral Structure Parameterization Technique: Retrieval of Total Water Vapor Columns from GOME, Atmos. Chem. Phys., 3, 145–160, 2003,
SRef-ID: 1680-7324/acp/2003-3-145. 7921, 7922, 7924, 7927, 7936

Lanzante, J. R., Klein, S. A., and Seidel, D. J.: Temporal Homogenization of Monthly Radiosonde Temperature Data, Part I: Methodology, J. Climate, 16, 224–240, 2003. 7935

Lawrence, M. G.: Photochemistry in the tropical pacific troposphere: Studies with a global 3D chemistry-meteorology model, PhD thesis, Ga. Inst. of Technol., Atlanta, 1996. 7933

Lawrence, M. G.: Evaluating trace gas sampling strategies with assistance from a global 3D photochemical model: Case studies for CEPEX and NARE O3 profiles, Tellus, 53B, 22–39, 2001. 7920

Lawrence, M. G. and Crutzen, P. J.: The impact of cloud particle gravitational setteling on soluble trace gas distributions, Tellus, Ser. B, 50, 263–289, 1998. 7920, 7934

Lawrence, M. G. and Crutzen, P. J.: Influence of NO_x emissions from ships on tropospheric photochemistry and climate, Nature, 402, 167–170, 1999. 7920

Lawrence, M. G., Crutzen, P. J., Rasch, P. J., Eaton, B. E., and Mahowald, N. M.: A model for studies of tropospheric photochemistry: Description, global distributions, evaluation, J. Geophys. Res., 104, 26 245–26 277, 1999. 7920, 7933, 7934

Hydrological cycle of MATCH

R. Lang and
M. G. Lawrence

Title Page

Abstract	Introduction
Conclusions	References
Tables	Figures

|◄ | ►|
◄ | ►

Back | Close

Full Screen / Esc

Print Version

Interactive Discussion

EGU

Lawrence, M. G., Rasch, P., von Kuhlmann, R., Williams, J., Fischer, H., Reus, M., Lelieveld, J., Crutzen, P., Schultz, M., Stier, P., Huntrieser, H., Heland, J., Stohl, A., Forster, C., Elbern, H., Jakobs, H., and Dickerson, R.: Global chemsitry weather forecasts for field campaign planning: Predictions and observations of large-scale features during MINOS, CONTRACE, and INDOEX, Atmos. Chem. Phys., 3, 267–289, 2003a, SRef-ID: 1680-7324/acp/2003-3-267. 7920

Lawrence, M. G., von Kuhlmann, R., Salzmann, M., and Rasch, P. J.: The balance of effects of deep convective mixing on tropospheric ozone, Geophys. Res. Lett., 30, 18, 1940, doi:10.1029/2003GL017644, 2003b. 7920

Learner, R., Schermaul, R., Tennyson, J., Zobov, N., Ballard, J., Newnham, D., and Wickett, M.: Measurement of H_2O Absorption Cross-Sections for the Exploitation of GOME data, ESTEC Contract No 13312/9/NL/SF, Final Presentation, 2000. 7919

Mahowald, N. M., Prinn, R. G., and Rasch, P. J.: Deducing CCl_3F emissions using an inverse method and chemical transport models with assimilated winds, J. Geophys. Res., 102, 28 153–28 168, 1997a. 7920, 7933

Mahowald, N. M., Rasch, P. J., Eaton, B. E., Whittlestone, S., and Prinn, R. G.: Transport of [222]radon to the remote troposphere using the Model of Atmospheric Transport and Chemistry and assimilated winds from ECMWF and the National center for Environmental Prediction/NCAR, J. Geophys. Res., 102, 28 139–28 152, 1997b. 7920, 7933

Maurellis, A. N. and Tennyson, J.: The climatic effects of water vapour, Physics World, May, 2003. 7919

Maurellis, A. N., Lang, R., van der Zande, W. J., Ubachs, W., and Aben, I.: Precipitable Water Column Retrieval from GOME Data, Geophys. Res. Lett., 27, 903–906, 2000a. 7922, 7924

Maurellis, A. N., Lang, R., and van der Zande, W. J.: A New DOAS Parameterization for Retrieval of Trace Gases with Highly-Structured Absorption Spectra, Geophys. Res. Lett., 27, 4069–4072, 2000b. 7924

Metzger, S. M., Dentener, F. J., Lelieveld, J., and Pandis, S. N.: Gas/aerosol Partitioning I: A Computationally Efficient Model, J. Geophys. Res., 107, D16, doi:10.1029/2001JD001102, 2002. 7919, 7951

Minschwander, K. and Dessler, A. E.: Water Vapor Feedback in the Tropical Upper Troposphere: Model Results and Observations, J. Climate, 17, 1272–1282, 2004. 7919

Naus, H. and Ubachs, W.: Visible absorption bands of the $(O_2)_2$-collision complex at pressures below 760 Torr, Appl. Opt., 38, 3423–3428, 1999. 7925

Hydrological cycle of MATCH

R. Lang and M. G. Lawrence

Title Page

Abstract | Introduction

Conclusions | References

Tables | Figures

◀ | ▶

◀ | ▶

Back | Close

Full Screen / Esc

Print Version

Interactive Discussion

EGU

Noël, S., Buchwitz, M., Bovensmann, H., Hoogen, R., and Burrows, J. P.: Atmospheric Water Vapor Amounts Retrieved from GOME Satellite Data, Geophys. Res. Lett., 26, 1841–1844, 1999. 7924

Noël, S., Buchwitz, M., Bovensmann, H., and Burrows, J. P.: Retrieval of Total Water Vapour Column Amounts from GOME/ERS-2 Data, Adv. Space Res., 29, 11, 1697–1702, 2002. 7924

Noël, S., Buchwitz, M., and Burrows, J. P.: First retrieval of global water vapour column amounts from SCIAMACHY measurments, Atmos. Chem. Phys., 4, 111–125, 2004, SRef-ID: 1680-7324/acp/2004-4-111. 7928

Peixoto, J. P. and Oort, A. H.: Physics of climate, American Institute of Physics, New York, 520pp, ISBN 0-88318-711-6, 1992.

Pfeilsticker, K., Erle, F., and Platt, U.: Absorption of solar radiation by atmospheric O_4, J. Atmos. Sci., 54, 933–939, 1997. 7925

Picone, J. M., Hedin, A. E., Drob, D. P., and Aikin, A. C.: NRLMSISE-00 empirical model of the atmosphere: Statistical comparisons and scientific issues, J. Geophys. Res., 107, A12, Art. No. 1468, 2002. 7925

Randel, D. L., Vonder Haar, T. H., Ringerud, M. A., Stephens, G. L., Greenwald, T. J., and Combs, C. L.: A new global water vapor dataset, Bull. Americ. Meteorol. Soc., 77, 6, 1233–1246, 1996. 7929

Rasch, P. J. and Kristjánsson, J. E.: A Comparison of the CCM3 Model Climate Using Diagnosed and Predicted Condensate Parameterizations, J. Climate, 11, 1587–1614, 1998. 7934

Rasch, P. J. and Lawrence, M. G.: Recent developements in transport methods at NCAR, in MPI Workshop on Censervative Transport Schemes, Rep. 265, 65–75, Max-Planck-Inst. Meteorol., Hamburg, Germany, 1998. 7934

Rasch, P. J., Mahowald, N. M., and Eaton, B. E.: Representation of transport, convection and the hydrological cycle in chemical transport models: Implications for the modeling of short lived and soluble species, J. Geophys. Res., 102, 28 127–28 138, 1997. 7920, 7933, 7934

Rossow, W. B. and Schiffer, R. A.: ISCCP Cloud Data Products, Bull. Am. Met. Soc., 72, 2–20, 1991. 7926

Rudolf, B.: Satellite-based global precipitation estimates and validation results, Satellite Application Facility Workshop on Climate Monitoring, Dresden, Germany, November 2000, Workshop Report, 140–149, EUMETSAT, Darmstadt, Germany, ISBN 92-9110-042-0, 2001.

Hydrological cycle of MATCH

R. Lang and
M. G. Lawrence

Title Page

Abstract	Introduction
Conclusions	References
Tables	Figures

◄ | ►►

◄ | ►

Back | Close

Full Screen / Esc

Print Version

Interactive Discussion

EGU

7923, 7930, 7931

Simpson, J. J., Berg, J. S., Koblinsky, C. J., Hufford, G. L., and Beckley, B.: The NVAP global water vapor data set: independent cross-comparison and multiyear variability, Remote Sesing of Environment, 76, 112–129, 2001. 7929

5 Slingo, J. M.: The developement and verification of a cloud prediction scheme for the ECMWF model, Q. J. R. Meterol. Soc., 113, 899–927, 1987. 7934

Stendel, M. and Arpe, K.: Evaluation of the hydrological cycle in reanalyses and observations, Max-Planck-Institut für Meteorologie, Hamburg, Germany, 52 pp, 1997. 7932, 7947

Stephens, G. L., Jackson, D. L., and Bates, J. J.: Acomparison of SSM/I and TOVS column
10 water vapor over the global oceans, Meteorology and Atmospheric Physics, 54, 183–201, 1994. 7929

Thomas, W., Hegels, E., Slijkhuis, S., Spurr, R., and Chance, K.: Detection of Biomass Burning Combustion Products in Southeast Asia from Backscatter Data Taken by the GOME Spectrometer, Geophys. Res. Lett., 25, 1317–1320, 1998. 7924

15 Tuinder, O. N. E., de Winter-Sorkina, R., and Builtjes, P. J. H.: Retrieval methods of effective cloud cover from the GOME instrument: an intercomparison, Atmos. Chem. Phys., 4, 255–273, 2004,
SRef-ID: 1680-7324/acp/2004-4-255. 7926

Trenberth, K. E. and Guillemot, C. J.: The total mass of the atmosphere, J. Geophys. Res., 99,
20 D11, 23 079–23 088, 1994.

von Kuhlmann, R., Lawrence, M. G., Crutzen, P. J., and Rasch, P. J.: A model for studies of tropospheric ozone and nonmethan hydrocarbons: Model description and ozone results, J. Geophys. Res., 108, D9, 4294, doi:10.1029/2002JD002893, 2003a. 7920, 7933, 7934

von Kuhlmann, R., Lawrence, M. G., Crutzen, P. J., and Rasch, P. J.: A model for studies
25 of tropospheric ozone and nonmethan hydrocarbons: Model evaluation of ozone related species, J. Geophys. Res., 108, D28, 4729, doi:10.1029/2002JD003348, 2003b. 7920

Vonder Haar, T. H., Forsythe, J. M., McKague, D., Randel, D. L., Ruston, B. C., and Woo, S.: Continuation of the NVAP Global Water Vapor Data Sets for Pathfinder Science Analysis, STC Technical Report 3333, Science and Technology Corporation Fort Collins, Colorado,
30 2003. 7929

Wagner, T., Heland, J., Zöger, M., and Platt, U.: A fast H_2O total column density product from GOME – validation with in-situ aircraft measurements, Atmos. Chem. Phys., 3, 651–663, 2003,

SRef-ID: 1680-7324/acp/2003-3-651. 7924, 7925

Wentz, F. J.: A well-calibrated ocean algorithm for special sensor microwave/imager, J. Geophys. Res., 102, C4, 8703–8718, 1997. 7928

White, G. and da Silva, A.: An intercomparison of surface marine fluxes from GEOS-1/DAS, ECMWF/ERA and NCEP/NCAR reanalyses, 9th Conf. On Interaction of the Sea and Atmosphere, 11–16 Jan. 1998, Phoenix, Az. Amer. Meteor. Soc., Boston, MA, 20–23, 1998.

Xie, P. and Arkin, P. A.: Global precipitation: A 17-Year monthly analysis based on gauge observations, satellite estimates and numerical model outputs, Bull. Americ. Meteorol. Soc., 78, 11, 2539–2558, 1997. 7930

Zhang, G. J. and McFarlane, N. A.: Sensitivity of climate simulations to the parameterization of cumulus convection in the Canadian Climate centre general circulation model, Atmos. Ocean, 33, 407–446, 1995. 7934

Hydrological cycle of MATCH

R. Lang and
M. G. Lawrence

Title Page

Abstract	Introduction
Conclusions	References
Tables	Figures

◄◄   ►►

◄   ►

Back   Close

Full Screen / Esc

Print Version

Interactive Discussion

EGU

Table 1. Absolute global, hemispheric and tropical mean values for WVC modelled by MATCH. WVC mean values for different cloud mask applied are shown together with their relative differences with respect to the full mean values.

	Global		30° N–90° N		30° S–30° N		90° S–30° S	
August 1996–1998	[cm]	[%]	[cm]	[%]	[cm]	[%]	[cm]	[%]
MATCH all ground pixels	2.46	100	2.16	100	3.73	100	0.98	100
MATCH with GOME cloud mask	2.16	87.95	1.89	87.69	3.14	84.05	1.08	110.11
MATCH with common cloud mask	1.87	76.12	1.64	76.10	2.80	75.10	0.76	77.20
January 1996–1998								
MATCH all ground pixels	2.13	100	0.81	100	3.58	100	1.37	100
MATCH with GOME cloud cover	1.90	89.60	0.91	112.69	3.0	84.72	1.3	94.69
MATCH with common cloud mask	1.64	77.01	0.69	85.69	2.69	75.14	1.06	77.70

R. Lang and
M. G. Lawrence

EGU

Table 2. Global and regional mean values for the WVC distributions as presented in Figs. 9 to 12, and for the precipitation rate (PR) comparisons presented in Figs. 13 to 17. In addition, the residence time (RT), given by the ratio of WVC over PR, is also denoted for all observed regions.

August 1996–1998	Global			Europe			Indian Ocean		
	WVC [cm]	PR [cm/day]	RT [day]	WVC [cm]	PR [cm/day]	RT [day]	WVC [cm]	PR [cm/day]	RT [day]
MATCH	2.17	0.40	5.42	1.95	0.32	6.08	3.48	0.75	4.64
NRA	2.37	0.37	6.41	2.09	0.22	9.49	4.07	0.76	5.35
GOME-SSP/GPCP	2.23	0.34	6.55	2.14	0.25	8.56	3.84	0.62	6.20
January 1996–1998									
MATCH	1.91	0.37	5.16	1.13	0.33	3.41	3.13	0.59	5.31
NRA	2.14	0.34	6.29	1.16	0.24	4.82	3.56	0.64	5.56
GOME-SSP/GPCP	1.92	0.33	5.81	1.00	0.35	2.84	3.30	0.52	6.35
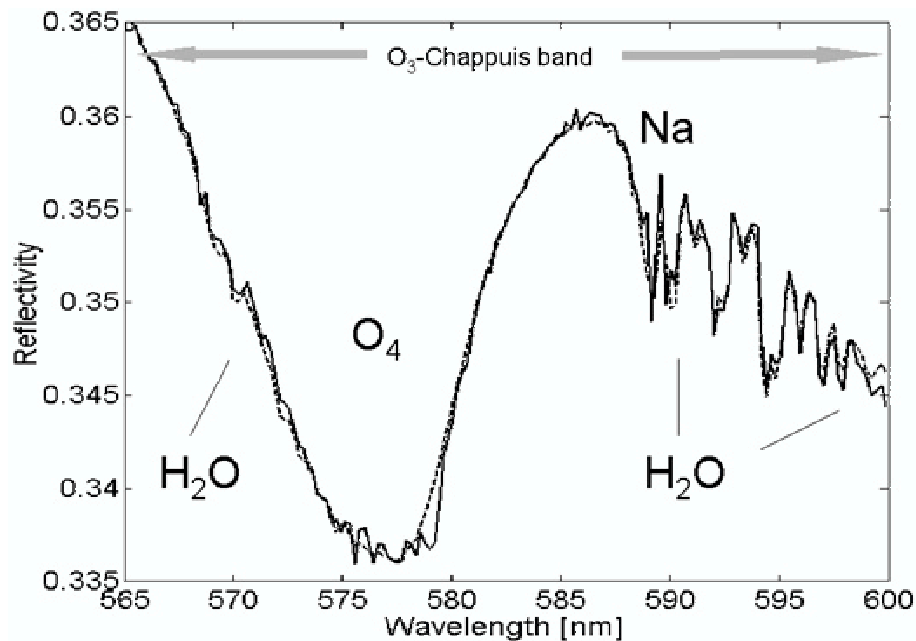
Fig. 1. GOME reflectivity spectrum (solid line) taken at 62° N (SZA=73°). The background consists of $(O_2)_2$, O_3 and Sodium. The stronger of the two $(O_2)_2$ absorption peaks is clearly visible around 577 nm with another WV absorption band between 565 and 580 nm superimposed on it. A fit to the spectrum using SSP is shown by the dashed line.

EGU
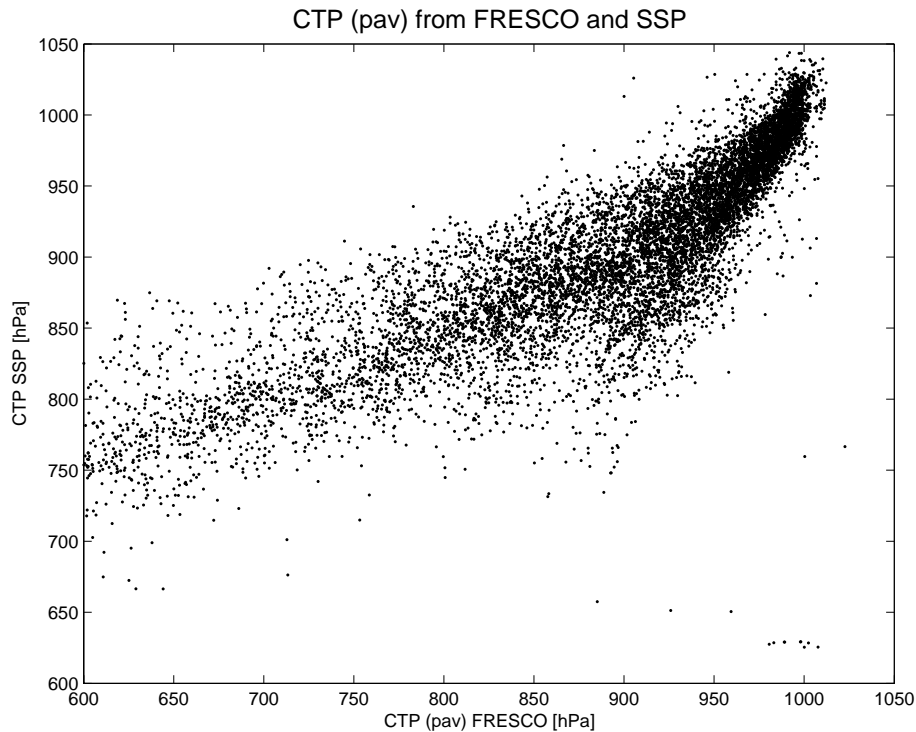
Fig. 2. Comparison between FRESCO derived cloud top pressure (CTP) and those derived from the SSP-$(O_2)_2$ retrieval scheme for 1 August 1998. Both retrievals are employing in total 14 GOME orbits of that day with retrievals restricted to SZA lower than 73°. The correlation is better than 75% (Pearson's r-square value) as is required for an accurate cloud-mask retrieval. However SSP-$(O_2)_2$ sees systematically lower clouds than FRESCO. FRESCO CTP values are weighted by the FRESCO derived cloud-fraction number per pixel to yield pixel averaged values (pav).

Title Page

Abstract   Introduction

Conclusions   References

Tables   Figures

◀◀   ▶▶

◀   ▶

Back   Close

Full Screen / Esc

Print Version

Interactive Discussion

EGU
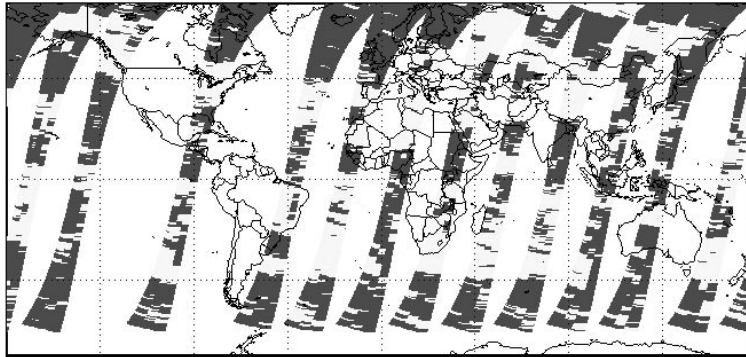
Cloud Mask from SSP

Cloud Mask from FRESCO
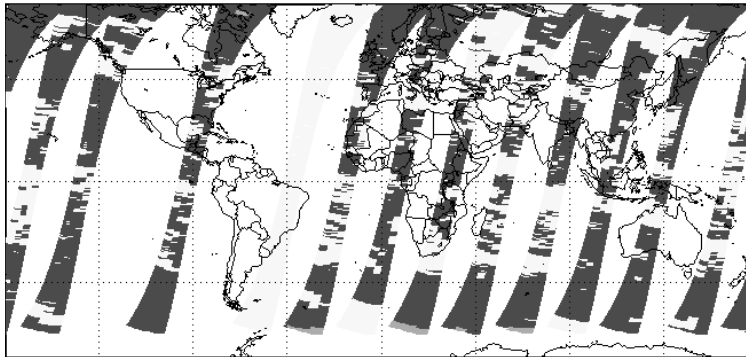
Fig. 3. SSP-$(O_2)_2$ derived cloud mask (upper panel) and the cloud mask derived from the FRESCO retrieval scheme (lower panel) for 1 August 1998. Cloud masked pixels are indicated in black for cloud fractions with more than 15% cloud cover. Cloud free scenes are indicated in white. Invalid cloud mask retrievals are indicated in light gray. FRESCO values for the GOME pass over the Atlantic and South America are missing for this day.

Title Page

Abstract Introduction

Conclusions References

Tables Figures

◄| |►

◄ ►

Back Close

Full Screen / Esc

Print Version

Interactive Discussion

EGU
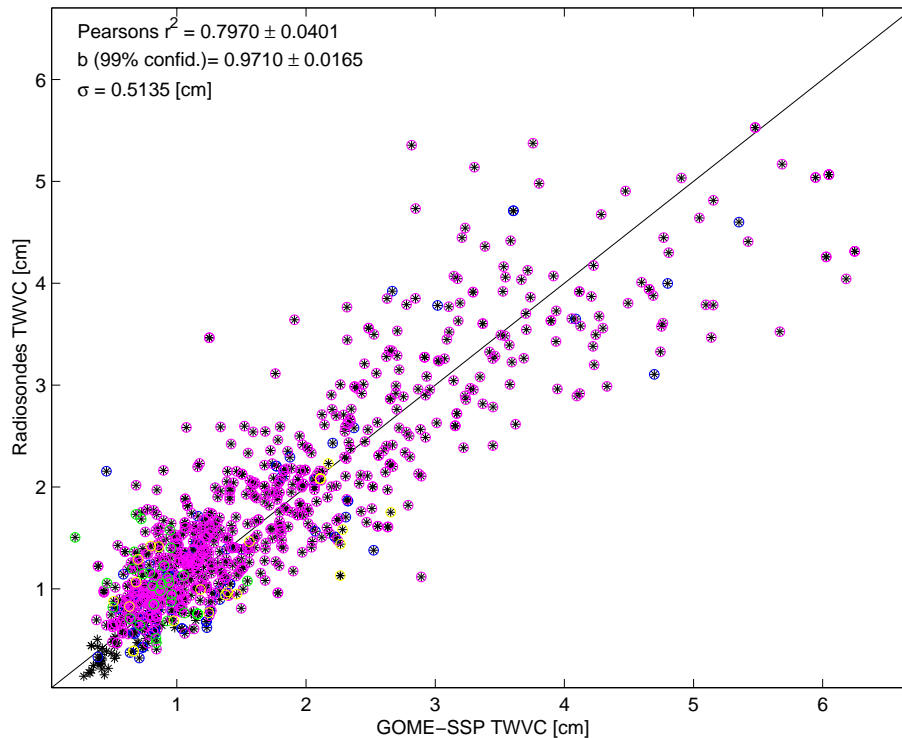
Fig. 4. Comparison between GOME WVC and radiosonde measurements from the ECMWF operational network for January and August 1995 to 2000. Values are correlated spatially and within 3 h in time. Pink and blue circles indicate Asian and Indonesian sondes, green circles indicate sondes from Europe, and yellow circles denote North American sonde values.

EGU
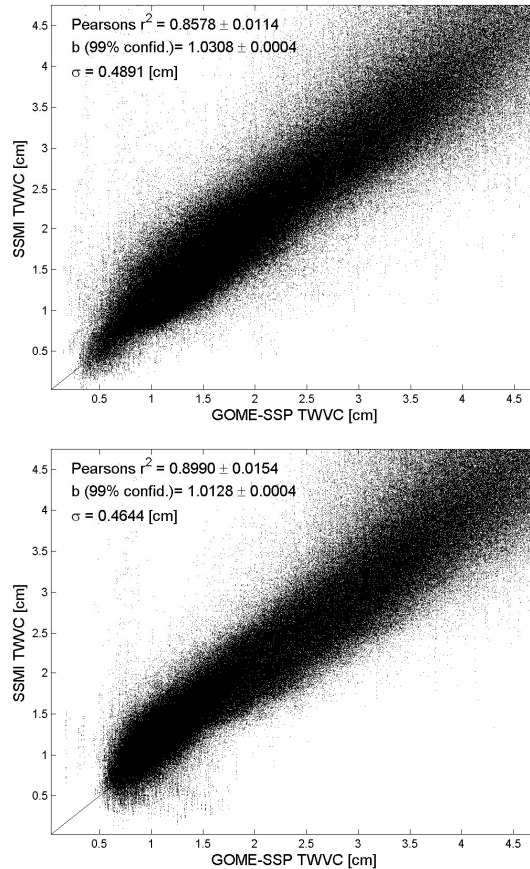
Fig. 5. Comparison between GOME WVC and those from the Special Sensor Microwave Imager on the Defense Meteorological Satellite Platforms F13 and F14 measurements for January (upper panel) and August (lower panel) 1996 to 1998. Values are correlated spatially and in time within 4 h until 1997 and 2 h after 1997.

Title Page

Abstract | Introduction

Conclusions | References

Tables | Figures

◄ | ►

◄ | ►

Back | Close

Full Screen / Esc

Print Version

Interactive Discussion

EGU

EGU
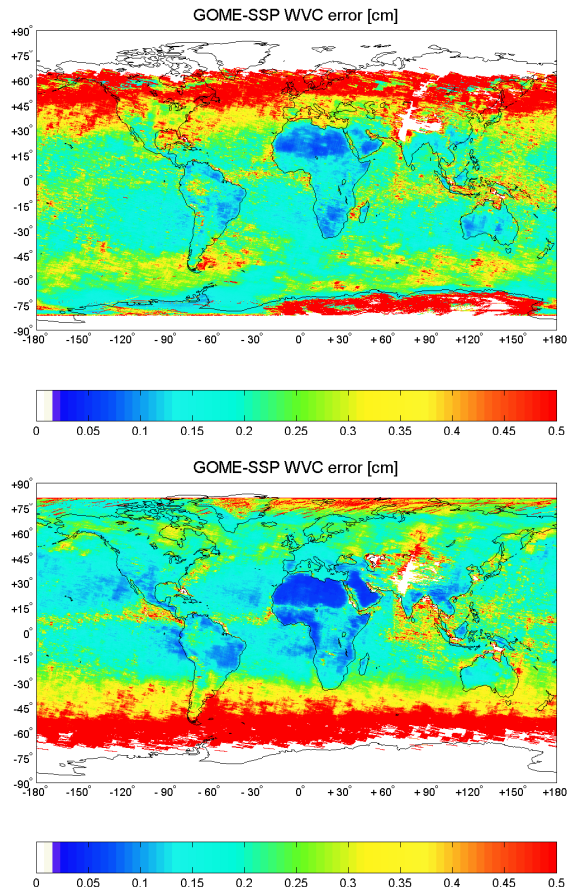
Fig. 6. GOME-SSP WVC total retrieval error for the monthly mean retrieved values of January (upper panel) and August (lower panel) 1996–1998. Missing values due to low statistics (high cloud frequency) or operational instrument calibrations (above Pakistan) are masked out and indicated in white. The relative error varies between below 5% along the ITCZ and over the subsidence region, 25% between 50 to 60 (30 to 40) degree and 50% and more above 70 (60) degree for hemispheric summer (winter).
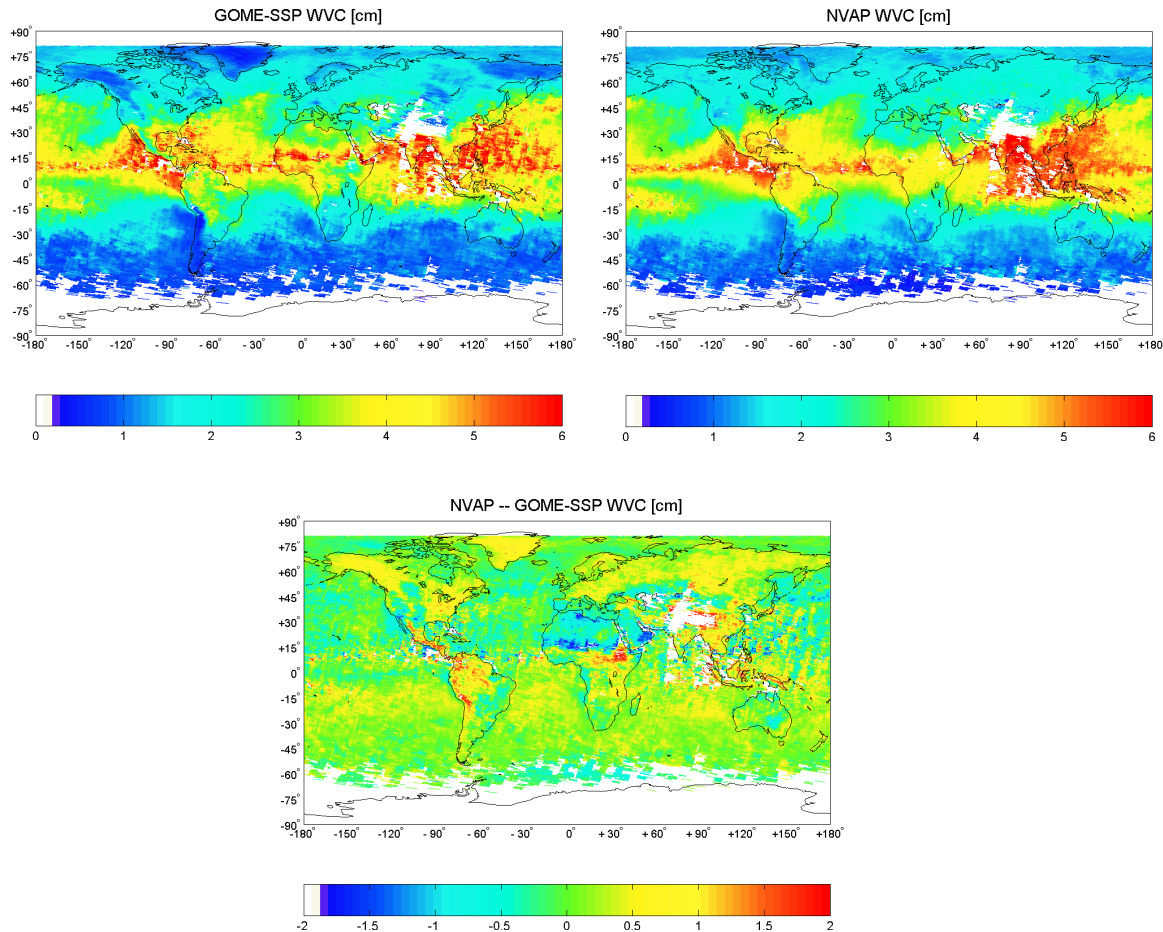
Fig. 7. Monthly averaged WVC for August 1998 from GOME (upper panel) and NVAP (middle panel). The lower panel shows the differences between the monthly mean values. The GOME retrieved cloud-mask is also applied to NVAP.
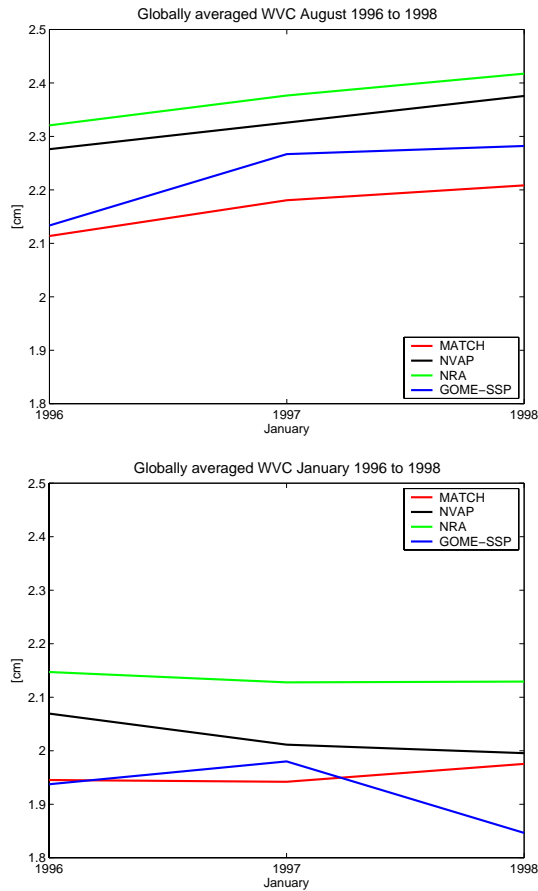
Title Page

Abstract   Introduction

Conclusions   References

Tables   Figures

◄   ►I

◄   ►

Back   Close

Full Screen / Esc

Print Version

Interactive Discussion

EGU

EGU
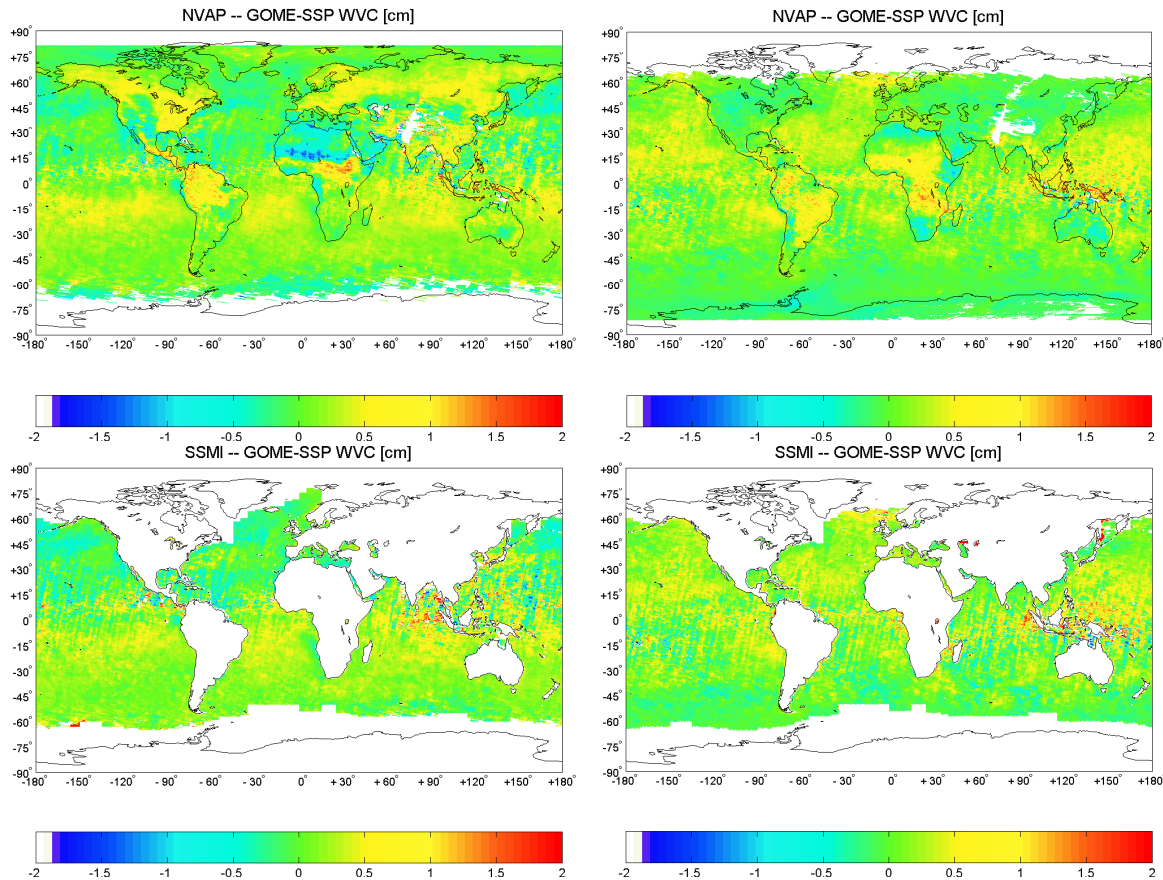
Fig. 8. Three years averaged WVC residuals for August (left panels) and January (right panels) 1996 to 1998 from GOME-SSP compared with NVAP (upper panels) and SSMI (lower panels) values. The GOME retrieved cloud-mask is applied to both products.

EGU
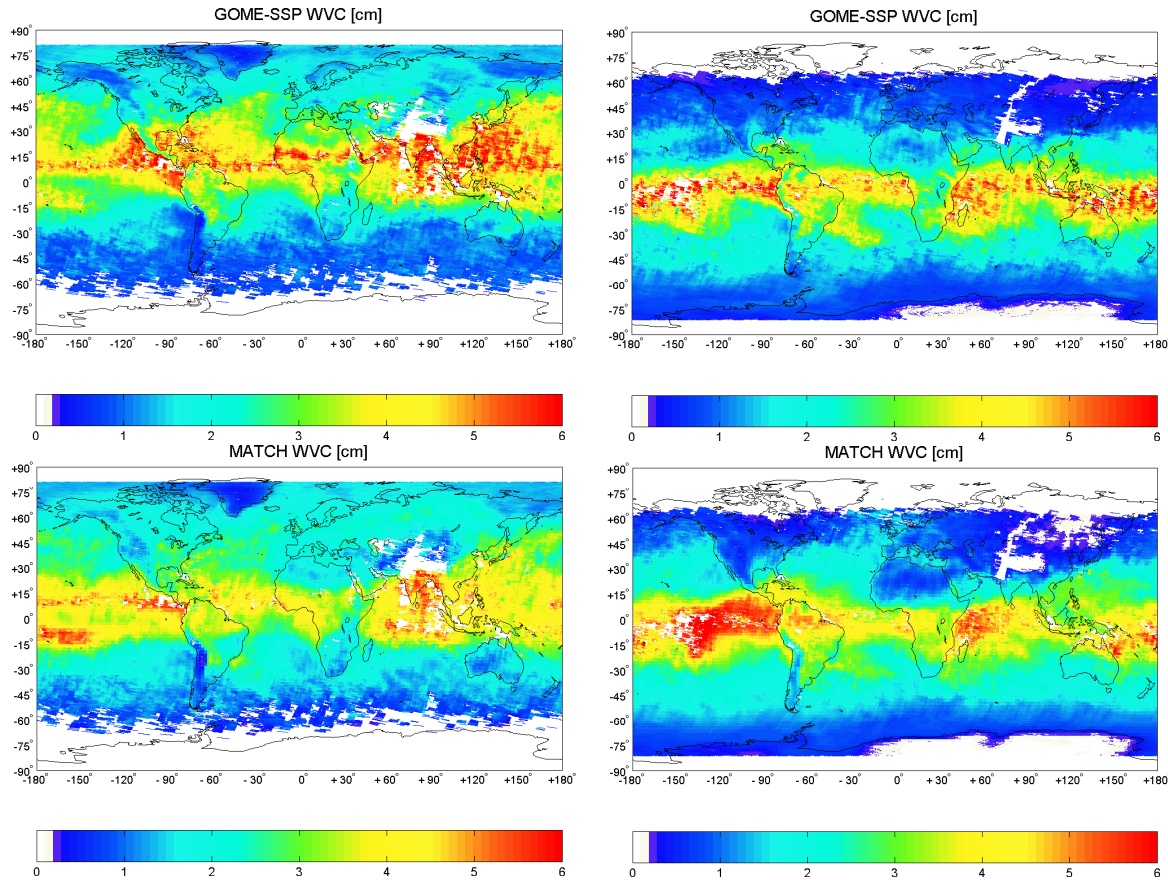
Fig. 9. Monthly averaged WVC for August (left panel) and January (right panels) 1998 from GOME (upper panels) and MATCH (middle panels). The lower panels show the differences between the monthly mean values. The GOME retrieved cloud-mask has also been applied to MATCH.

Hydrological cycle of MATCH

R. Lang and
M. G. Lawrence

Print Version

Interactive Discussion

EGU
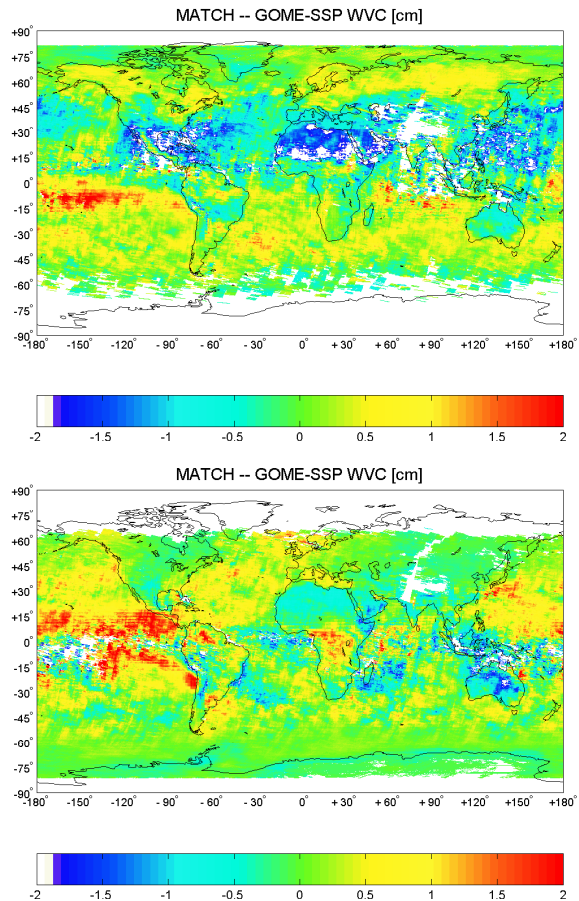
Fig. 9. Continued.

Hydrological cycle of MATCH

R. Lang and
M. G. Lawrence

Title Page

Abstract | Introduction

Conclusions | References

Tables | Figures

◄ | ►

◄ | ►

Back | Close

Full Screen / Esc

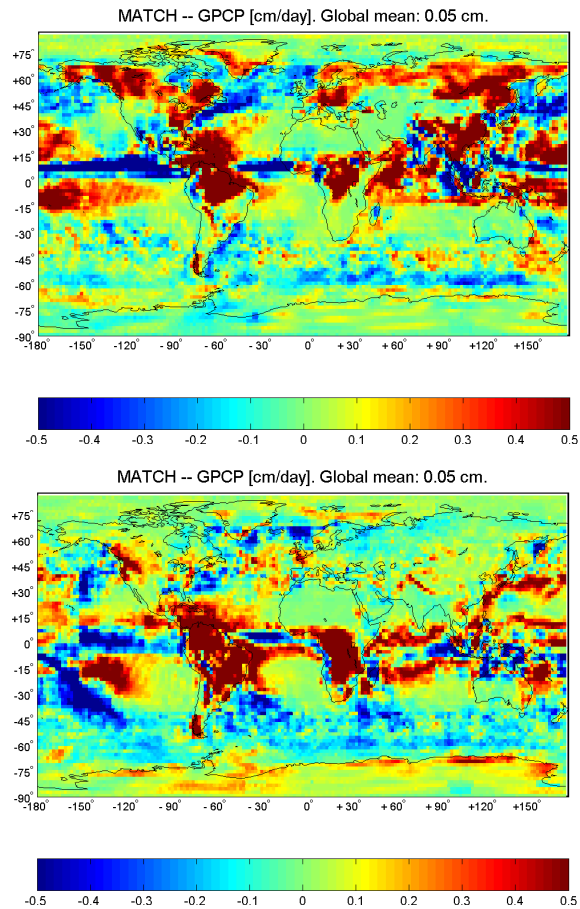Print Version

Interactive Discussion

EGU
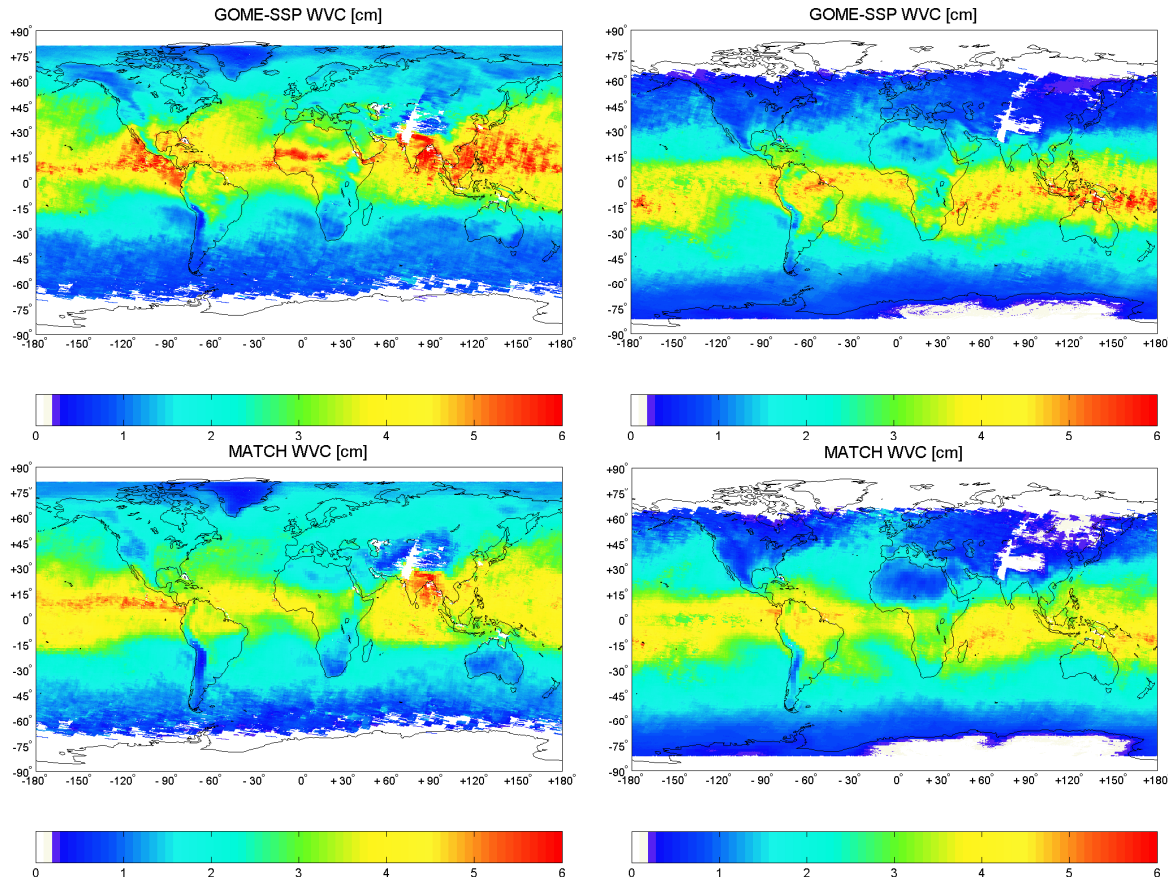
Fig. 10. Three years averaged WVC for August (left panel) and January (right panels) 1996 to 1998 from GOME (upper panels) and MATCH (middle panels). The lower panels show the differences between the three years averaged mean values. The GOME retrieved cloud-mask has also been applied to MATCH.

Fig. 10. Continued.

EGU
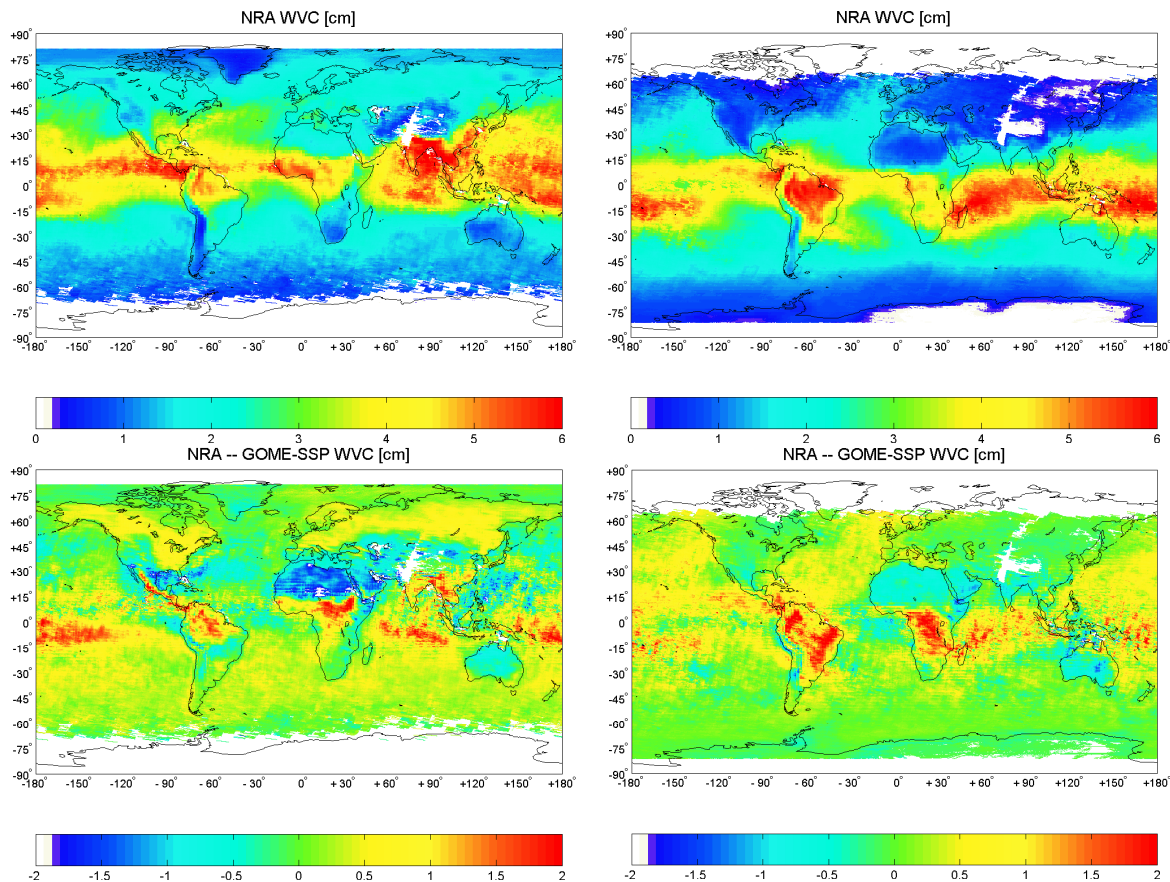
Fig. 11. Same as Fig. 10 but for WVC from NRA. The GOME retrieved cloud-mask has also been applied to NRA.

EGU

Fig. 12. Comparisons between zonally and globally averaged WVC from GOME-SSP, MATCH, NVAP and NRA. Zonally averaged WVC are given for for August and January 1998 (upper panels) and averaged over August and January 1996 to 1998 (middle panels). Global mean WVC are given in the lower two panels for August and January 1996 to 1998. All quantities are derived from the WVC distributions presented in Figs. 9 to 11.

Title Page

Abstract | Introduction

Conclusions | References

Tables | Figures

|◄ | ►|

◄ | ►

Back | Close

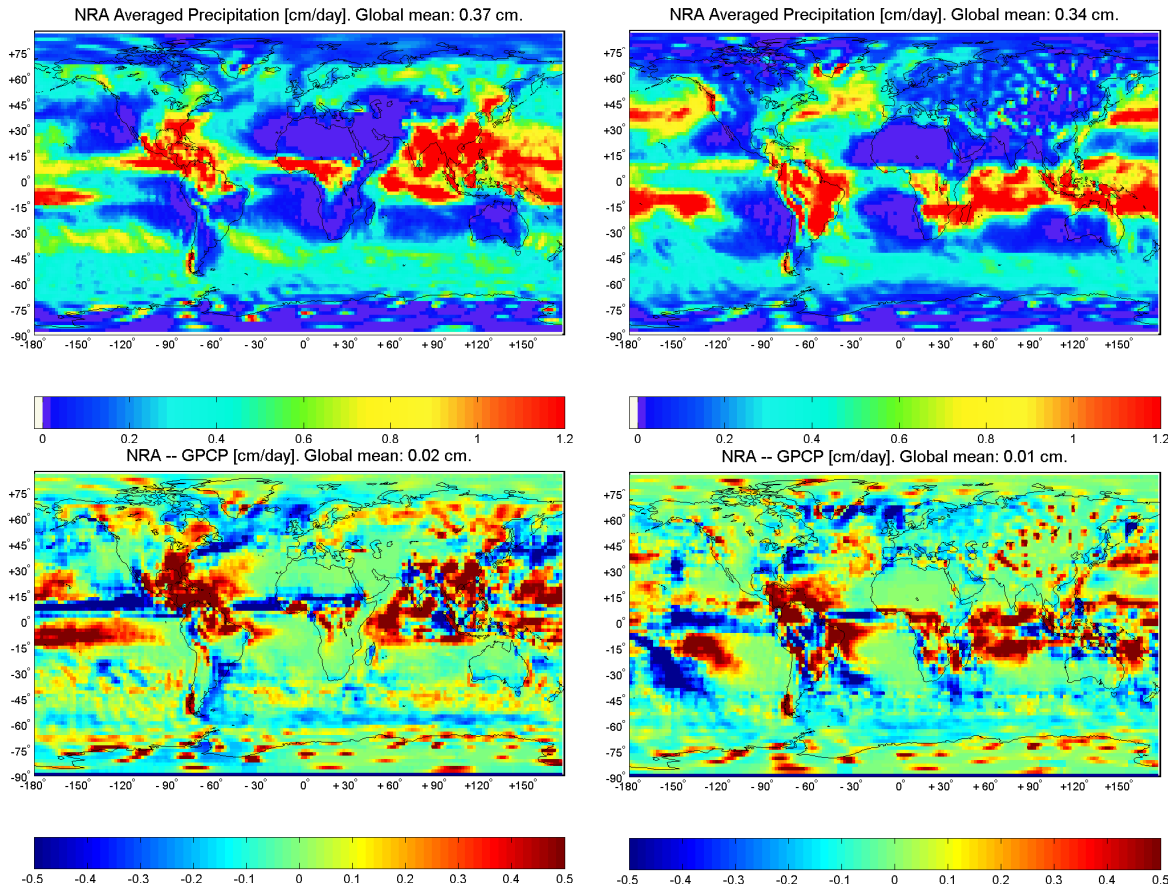Full Screen / Esc

Print Version

Interactive Discussion

EGU

Fig. 12. Continued.

EGU

Fig. 13. Global distribution of precipitation averaged over three years for August 1996 to 1998 (left panels) and January 1996 to 1998 (right panels). We compare daily precipitation amounts as provided by GPCP (see Sect. 3; upper panels) and as modelled by MATCH (middle panels). The differences between both products are given in the lower panels.

EGU

MATCH -- GPCP [cm/day]. Global mean: 0.05 cm.

MATCH -- GPCP [cm/day]. Global mean: 0.05 cm.

Fig. 13. Continued.

Title Page

Abstract | Introduction

Conclusions | References

Tables | Figures

◄ | ►

◄ | ►

Back | Close

Full Screen / Esc

Print Version

Interactive Discussion

EGU

Fig. 14. Same as Fig. 13 but for NRA results in comparison to GPCP.

Contribution of convective precipitation [%]

Contribution of convective precipitation [%]
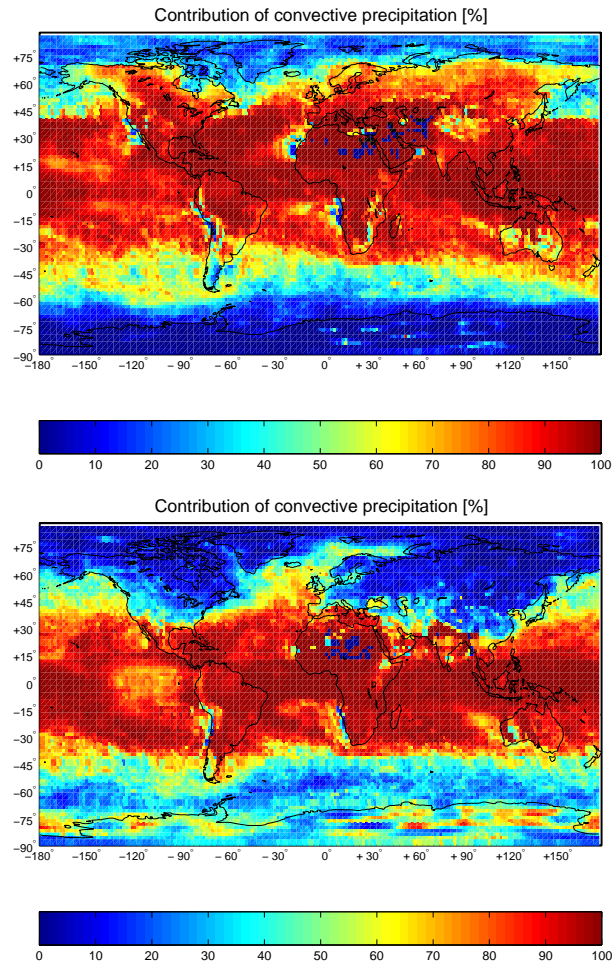
Fig. 15. Averaged relative contribution of convective to the total (large-scale plus convective) amount of precipitation as modelled by MATCH for August (upper panel) and January (lower panel) 1996 to 1998.

EGU
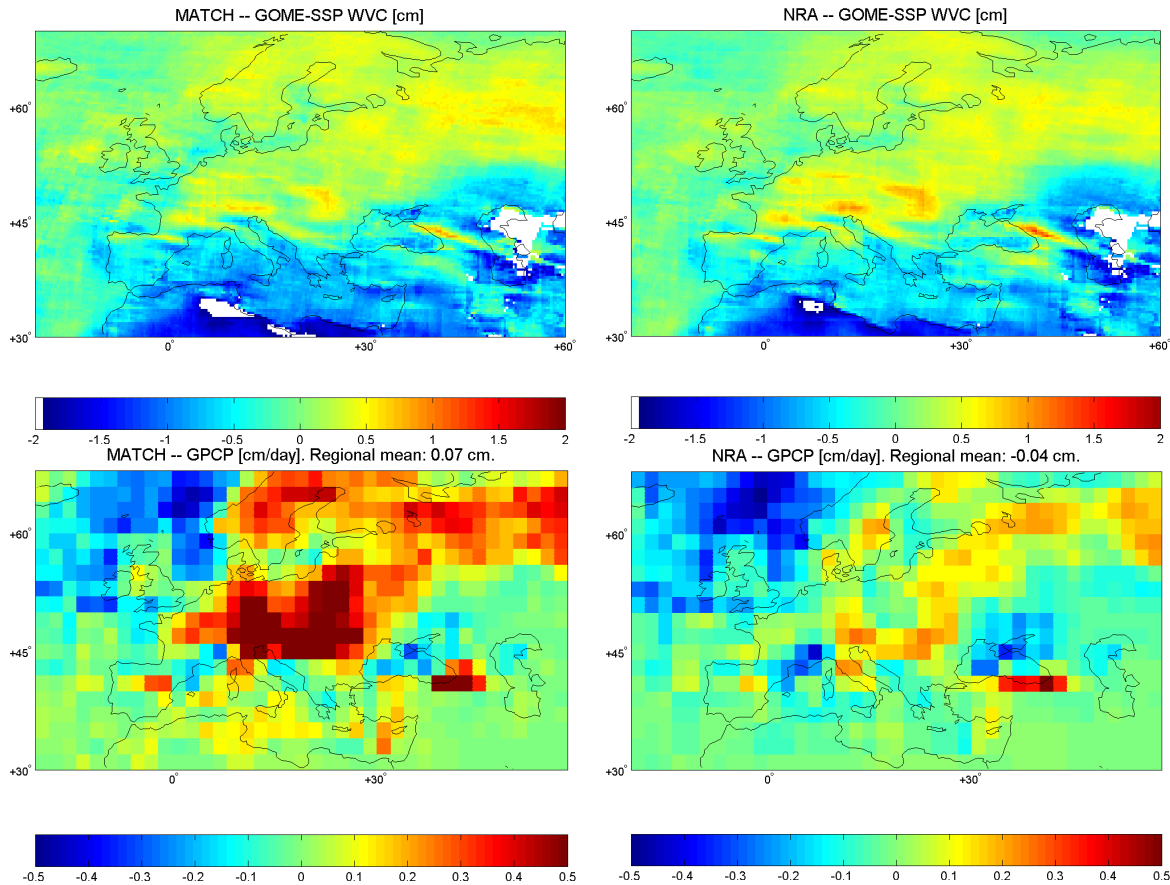
Fig. 16. Differences between MATCH (left panels) and NRA (right panels) modelled WVC and GOME-SSP WVC (upper panels) over Europe and for August 1996 to 1998. The lower panels show the corresponding residuals between the modelled precipitation amounts and those given by the GPCP observational data set over the same area and for the corresponding time period.
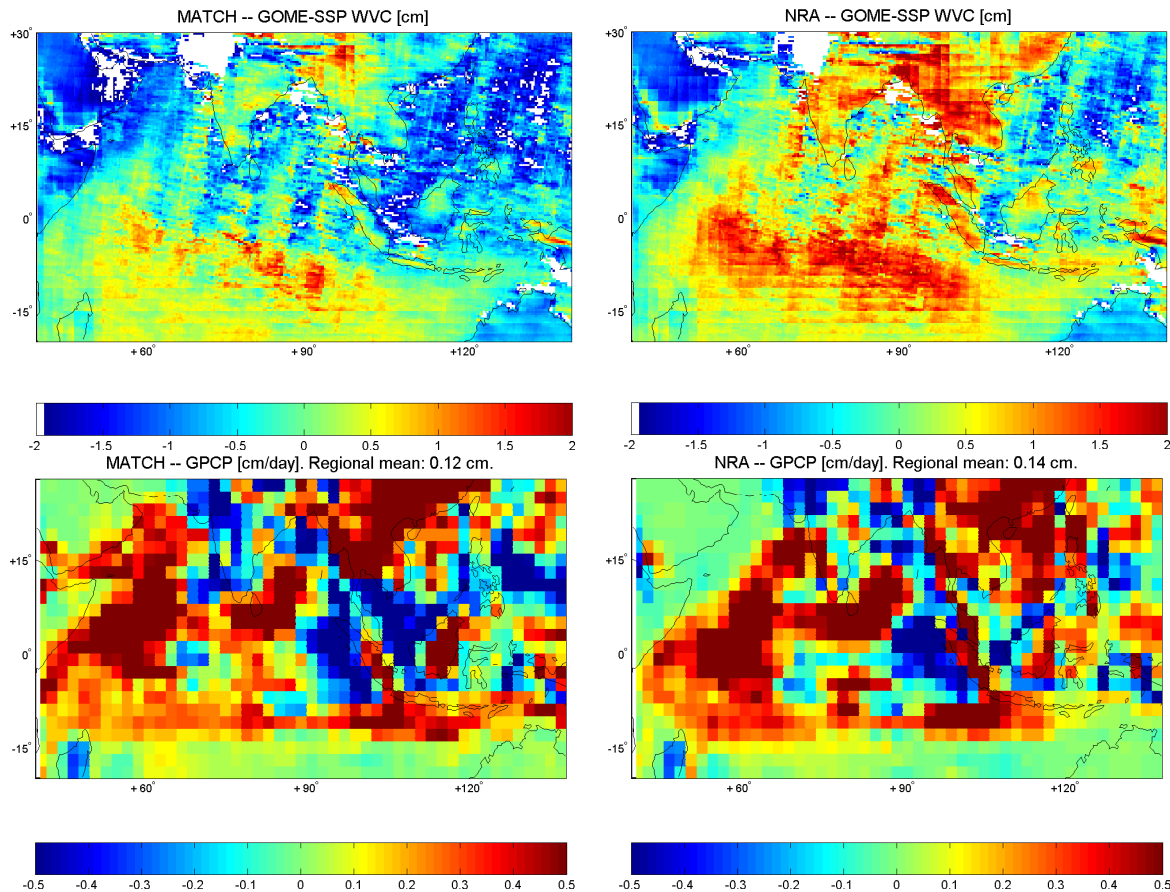
Fig. 17. Same as Fig. 16 but for Southern Asia and the Indian Ocean region.

EGU